A BIOPHYSICAL CONDUCTANCE-BASED MODEL OF NEURAL SPIKE TIMING AND INTERSPIKE INTERVAL CORRELATIONS

BY

ALEXANDER ASILADOR

DISSERTATION

Submitted in partial fulfillment of the requirements
for the degree of Doctor of Philosophy in Neuroscience
in the Graduate College of the
University of Illinois Urbana-Champaign, 2023

Urbana, Illinois

Doctoral Committee:

Professor Rama Ratnam, Chair
Professor Douglas L. Jones, Co-Chair
Professor Daniel A. Llano
Assistant Professor Benjamin D. Auerbach

Abstract

Neurons encode information in the form of spike times. It is argued that the timing between spikes (i.e., spike-timing) encodes the stimulus input. Spike threshold adaptation is speculated to be the major driving force behind a spike-timing code. Efforts to understand the neuron channels that drive an adaptive threshold have relied on purely mathematical models. Such models have had great success at predicting spike times [1], [2], but do not have a strong basis in biophysics or what is known about neural channels to predict spike timing. State-of-the-art biophysical models, however, suffer at the cost of model interpretability and spike-timing accuracy. We investigate spike threshold adaptation with a biophysical, Hodgkin-Huxley type model in a reduced fashion, with consideration to voltage-gated ion channels present only the axonal hillock, and fit spike timing that outperforms the best phenomenological model. We then evaluate the presence and effect of spike-threshold adaptation by estimating the current-voltage interaction and determine that the Kv7/KCNQ ion channel is likely the major ion channel responsible for an adaptive threshold in rodent pyramidal cells *in-vitro*. These findings are an alternative approach to previous research investigating outward potassium channels, and partially agree with previous research. We next develop a stochastic extension of the model with consideration of other stochastic models to produce stochastic spike timing and behavior observed in experimental data. We find that a stochastic Kv7/KCNQ ion channel with correlated spike-to-spike noise is able to reproduce neuron variability in experimental data and is consistent with the theoretical parameters derived from a stochastic dynamic threshold model.

This thesis is dedicated to my parents, for their endless support

Acknowledgments

My research was supported by an NSF-IGERT fellowship (IGERT-0903622), and research grants from the University Research Board (Ahmedabad University), and College of Engineering, and Coordinated Science Laboratory (UIUC), and the Advanced Digital Sciences Center (Illinois at Singapore).

I would like to thank Professor Daniel Llano for inviting me to his lab meetings, offering a level of work atmosphere, and giving me one of my first opportunities in collaboration when I first arrived on campus. To his watchful eye and keeping in-check on my graduate school progress when there was uncertainty. To the present and former members of the Llano Lab, thank you for dealing with my endless curiosity.

To the members and past members of the Douglas L. Jones Lab: Long Le, Duc Phan, Erik Johnson, David Lee, David Cohen, Brantley Sturgeon, Michael Friedman, and Cagdas Tuna. To Jamie Norton, a former Neuroscience student. Thank you all for your guidance throughout the years, directly and indirectly. I've eagerly tried to soak every bit of knowledge the first time I had stepped into the Jones' student office, and my inspiration for learning has never ceased.

To all my friends in the University of Illinos. I'm forever grateful for the opportunity to meet and learn with you throughout the years. To my board game and tabletop game group, hosts Liran and Helen, for your friendship and for briefly taking my mind off research.

To the Neuroscience Program, current and former members: Stephanie Pregent, Sam Beshers, and Michelle Tomaszycki. Thank you for your support during my stay in the program.

Most importantly, I am eternally grateful to Professor Rama Ratnam and Professor Douglas L. Jones for their patience in advising me throughout the years and for never giving up on me, even when I would fail.

Table of contents

List of Figures

List of Abbreviations

ACSF	Artificial Cerebrospinal Fluid
AIS	Axonal Initial Segment
DC	Direct current
HH	Hodgkin Huxley Model
MHH	Minimum Hodgkin Huxley Model
INCF	International Neuroinformatics Coordinating Facility
ISI	Inter-spike interval
I-V	Current-Voltage
K_A	Transient A-type Potassium Current
K_{DR}	Potassium Delayed Rectifier
K_M	M-type (Muscarine) Potassium
kSamples	kiloSamples
MAT	Multiadaptive threshold
ms	milliseconds
mV	millivolt
MCMC	Markov Chain Monte Carlo
Na_P	Persistent Sodium Current
Na_v	Voltage-gated Sodium Channel
Na_T	Transient Sodium Current
pA	picoAmpere
V_m	Membrane Potential

List of Symbols

ρ_1	Serial correlation coefficient at lag 1
Γ	Coincidence Metric
Γ_A	Coincidence Metric normalized to the average between-trial coincidence in experimental data
ϵ_n	White Noise Process for the nth spike

Chapter 1

Introduction

Encoding is the method by which neurons translate information they receive into a series of action potentials, also known as a spike train. Throughout the literature, there is evidence of different encoding schemes in the brain. Specialized neurons attuned to a particular feature or pattern have been observed, such as phase coding in the hippocampus. From the perspective of a single neuron, there are two competing ideas: information is carried in the timing of individual spikes (temporal code), and information is carried in the aggregate rate of spikes (rate code). Despite several decades of research both, ideas are still debated. From the efficiency standpoint, there are arguments for both sides [3], [4]. Encoding, in the case of neuron-to-neuron communication, is when information arrives in synapses and is translated into a series of action potentials. Decoding is the field that centers around understanding information about the presynaptic neuron's input from the spikes. As early as the work of De Boer, (white noise approach), given an output of a neuron (action potentials), it has been shown that it is possible to approximately reconstruct the input using a linear filter [5]. In De Boer's work, auditory nerve fiber action potentials were recorded in the cat, and repeated trials of white noise stimulus were played in ears. The resulting spikes were averaged and the correlation between the spikes and sound input were calculated. The resulting transfer function estimates the firing rate, given the white noise stimulus. In terms of neural coding,

mathematical models have been formulated to capture the relationship between the input of a neuron and the spike trains it produces. One of the earliest models is the Leaky Integrate and Fire model (for review, see [6]), where the membrane voltage is treated as a low-pass circuit and outputs a spike when a threshold is reached, resetting to the resting voltage immediately.

Such spiking models can be purely phenomenological or biophysical. In terms of decoding, the idea of estimating the input stimulus of a neuron from a spike train of a neuron population was one of the earliest works in the field [7]. The study of decoding was applied to the input of a single neuron, named stimulus reconstruction. Stimulus reconstruction arose for single neurons [8] in the *Calliphora erythrocephela* visual system (see [9] for review). Apart from the work in stimulus reconstruction, the field of neural decoding largely refers to work at a population level.

Both scientific and pragmatic interests motivate our research into more advanced spiking models. Motivation: Efforts in studying neural coding not only help our understanding of sensory coding, but optimal signal detection strategies learned from neural coding can also be applied to improve brain machine interfaces and in low-power computing.

Chapter 2 serves as the background of neural encoding at the single neuron level, the spiking models frequently used by researchers, ion channels, and progress in the field of neural coding at a single neuron level. The aim of Chapter 3 is the introduction of the Hodgkin-Huxley type model capable of accurately producing spike times to partially explain elements of optimal source coding. The model is then extended in Chapter 4 to reproduce spike jitter present in real neurons under repeated stimuli. The stochastic form of the model is based on biophysical processes that extend beyond channel noise and proposed in its simplest form to be an outcome of ion channel modulation. This thesis is inspired by work from Jones and colleagues' [10], [11] derivation of optimal source coding in neurons. From mathematical first principles they derive an optimal neural timing code and demonstrate that it produces remarkably good fits to experimental spike train timing data. While accurate in terms of timing reproduction, this abstract mathematical model provides little guidance in

terms of its biophysical implementation in neuronal cells. The aim of this dissertation is to produce a biophysically plausible neuron model that accurately predicts spike timing and jitter in experimental data. I implement a minimum channel Hodgkin Huxley-type model fitted to a publicly available dataset [2] in rat layer 5 cortical pyramidal cells to reproduce firing behavior and infer insights of a dynamic threshold model.

Chapter 2

Background

2.1 Ion channels in the axon initial segment

During an action potential, a sequence of ion channels open and close to rapidly depolarize the neuron to create a pulse in the membrane potential. This sequence was first speculated by Julius Bernstein in 1912. The types of ion channels and their kinetics throughout the time of the action potential were conjectured by Hodgkin and Huxley in 1952. At the time, ion channels were only known as 'sodium' and 'potassium' channels. It was through the discovery of the patch clamp technique and gene sequencing that families of ion channels were classified. In the potassium channel family alone, there are 180 different genetic expressions, all of which produce different kinetics [12]. These channels are termed voltage-gated ion channels, which are a superfamily of ion channels that open and close based on a cell's membrane potential. Ligand-gated ion channels, on the other hand, are modulated by chemical binding. While voltage-gated ion channels open primarily by membrane potential, there exist channels in this superfamily that are additionally modulated by various ligands to alter their kinetics. One example is the KCNQ2/3 channel, which closes based on the concentration of Acetylcholine [13]. The ionic channels in the mammalian neuron vary by the neuron's location. For clarity, the following notations for each channel are based on those consistent with the literature

in biophysical modeling of neurons [14]–[17], rather than their genetic classification. While there is a relationship to the genetic classification and its membrane physiology, under certain conditions, its kinetics across different organs and species can lead to a categorically different physiology in some ion channels [18]–[20].

The channels involved in the action potential have been first speculated to occur in the axon hillock, a region in the axon proximal to the soma. Evidence in fluorescent channel labeling is that action potentials begin in the distal area of the Axonal Initial Segment (AIS) [21]–[23]. In this region, there is a large expression of Nav1 (Na_T and Na_P), delayed rectifier (K_D), transient potassium (K_A) and Kv7.2/7.3 channels (K_M) [15]. An extensively studied neuron used in mammalian physiology are the layer 5 pyramidal cells in the neocortex. It is one of the neurons that receive dendritic input from all layers in the cortex [24], [25], and send long range output to many areas in the brain, including sub-cortical structures [26]–[28]. They can be categorized by their anatomy as thick-tufted or slender-tufted. Thick-tufted layer 5 neurons have apical dendrites in the superficial layers and are characterized as intrinsic bursting cells in mature rodents. Slender-tufted layer 5 neurons project to layers 2/3 and have a regular spiking behavior [26]. The interest in this neuron is its association with sensory processing as well as its implication in pathophysiology, such as epilepsy and schizophrenia [15].

2.2 Neuron Spiking Models

Regarding neural spiking models used for understanding neural coding, I will discuss the single neuron models that have been used to investigate spiking behavior such as biophysical mechanisms and spike-timing. The most-known are the Hodgkin-Huxley and Integrate-and-Fire models. The former relates the dynamics of voltage-gated ion channels to spiking, and the latter describes the firing behavior to the summed input of the neuron. In addition to the models above, there are variants from the original equations due to increasing knowledge of

ion channels and their kinetics, mathematical analysis of dynamical systems, and to reduce computational complexity. Since 1952, many other types of voltage-gated ion channels that influence the spiking behavior have been discovered. Spike-frequency adaptation, being one of such behaviors, has attributed to certain ion channels and have been implemented in spiking models. Modelers have approached spike frequency adaptation in two different ways, either by using an adaptive current's kinetics directly, or by adding a mathematical equation that changes the "threshold" of the neuron after a spike fires. Multi-compartment models and morphological models are another class of models that factor in compartmentalization, which influence the membrane potential. Along with what I will describe, there are many more neuron spiking models beyond the scope of this thesis.

2.2.1 Hodgkin Huxley-type models

The Hodgkin-Huxley model [29] was introduced by Alan Hodgkin and Andrew Huxley as an effort to understand the ionic mechanisms responsible for the action potential in the giant squid axon. Its use in trying to understand ion channel dynamics has been very popular in computational groups. The formulas describing the Hodgkin-Huxley model are based on voltage-clamp data in the giant squid axon. At the time, sodium and potassium channels were speculated to be involved in the action potential.

$$C\frac{dV}{dt} = \bar{g}_{Na}m^3h\left(V - V_{Na}\right) + \bar{g}_K n^4\left(V - V_K\right) + \bar{g}_L\left(V - V_L\right)$$

$$\frac{dx}{dt} = \alpha_x\left(1 - x\right) - \beta$$

where x refers to the dynamics of the gating variable (m, h and n). $\alpha\left(V\right)$ and $\beta\left(V\right)$ are the voltage-dependent open and closing rates of a subunit in an ion channel, and $\bar{g}_x$ is the maximum conductance of a channel. L refers to a leak conductance, an ohmic conductance that establishes the resting membrane potential. In the equation above, the sodium current gating variable is m^3h to represent the interaction of activation subunits m, and inactivation

h.

Alternatively, the equations of the gating variables can be expressed as a change in the steady state of its gating over time with the expressions:

$$\frac{dx}{dt} = \frac{x - x_\infty(V)}{\tau(V)}$$

$$x_\infty = \frac{\alpha(V)}{\alpha(V) + \beta(V)},\ \tau = \frac{1}{\alpha(V) + \beta(V)}$$

In further work the Hodgkin-Huxley model has been modified in various ways, from inclusion of ion channels not originally present in the model to simplifications of the model that preserve the ion dynamics but reduce the computational complexity or analysis (such as the Morris-Lecar Model or Fitzhugh-Nagumo model), and termed Hodgkin Huxley-type models.

2.2.2 Integrate and Fire models

Models of this type treat the membrane potential as an integrator of the neuron's input. The Leaky Integrate-and-Fire model treats the current-voltage relationship as strictly linear

$$\tau \frac{dV}{dt} = RI(t) - [V(t) - V_{rest}]$$

where R is the membrane resistance, $I(t)$ is the injected current, $V(t)$ is the membrane voltage, and τ is its time constant.

The change in voltage in membrane potential is determined by the input current, the membrane resistance, and the driving force created by the membrane potential at time t against its resting membrane potential. When the voltage reaches a threshold V_{thresh}, in the integrate and fire model, the driving force is $V(t) - V_{rest}$. However, the driving force can be treated as a function that relates the behavior to that seen in neurons. The current-voltage relationship in the membrane can be defined by replacing $V(t) - V_{rest}$ with a function $f(u)$ defining this relationship [30]. These so-called Generalized Integrate-and-Fire Models have

been used to fit experimental data [31], [32]. Further, the equations that represent the function of the spiking output can be generalized, with a combination of linear filters instead of differential equations, to produce a transfer function. Combined with a rectified nonlinear operation, the termed spike-response model (SRM) or generalized linear model (GLM) [33], [34] is a phenomenological model widely used to model spiking behavior (for review, see [30]).

2.2.3 Adaptation Current Models and Dynamic Threshold models

Adaptation current models are those that incorporate the dynamics of those channels that are known to be involved in spike-frequency adaptation. These types of models can be applied to the Hodgkin-Huxley or Integrate-and-fire models to introduce spike-frequency adaptation into the spiking model. Since adaptation current models use the channel dynamics to produce the desired spiking behavior, the resulting model results in a nonlinear term caused by the channel dynamics themselves. Dynamic threshold models, on the other hand, treat the threshold term in the Integrate-and-fire models as a variable that changes based on the previous spiking history, and is typically modeled as a phenomenological function to incorporate a linear change in current [35]. Dynamic threshold models have been successfully used to predict spike timing experimental *in-vitro* neuron recordings [1], [36]. In 2009, Kobayashi's multiadaptive threshold model (MAT) won the International Neuroinformatics Coordinating Facility (INCF) spike time prediction challenge. The MAT model has related parameters in the model's dynamic threshold to the M-current and calcium-activated potassium current [1] from its dynamic threshold, and suggests that it may be possible to predict spike times with a Hodgkin Huxley-type model.

2.2.4 Multicompartment/Morphological models

In Hodgkin-Huxley type models, it has been shown that compartmentalization of the equations into separate dendrite and soma structures are capable of altering membrane potential and can produce behavior seen in experimental data [37], [38]. Recently, biophysical models have

included highly detailed morphology of a neuron to fit spiking behavior [17], [39]. In their work, features from firing behavior, such as timing, spike frequency, adaptation index and ISI covariance are extracted, and a multi-objective optimization procedure is used for fitting. The procedure for these models would normally have a very large set of free parameters to fit, but efforts to reduce the parameter space, such as altering only maximum conductance parameters and treating each compartment in a location as homogeneous, can effectively reduce the number of free parameters [40]. Recent models that have emerged for the rat layer 5 pyramidal cells include the Schaefer [41], Hay [17], and Almog [42] models. However, a comparison of such models shows that they are good at replicating behavior at the compartment it was fitted for, for example in the soma, but less representative in other regions, such as the axon initial segment and the dendrites [43].

2.3 Progress in Neural Encoding

Researchers in neural coding have argued whether the timing between spikes or the firing rate represent the information. Rate coding is the view that information is encoded in the firing rate [44]. At the population level, the ideas behind rate-coding are well-defined and have been used to describe H1 visual neuron response to looming stimuli in the fly [45], [46] and V1 neurons in the macaque [33].

In the single neuron level, rate coding is less defined since the timescale of the rate can be arbitrary in models. For this section, I will focus on research in neural encoding at the single neuron level. Early researchers in physiology had taken interest in the distribution in the timing between discharge patterns in muscle fibers, with some suspecting that the distribution is caused by a stochastic process [47]. One behavior noticed in such recordings was negative correlations between consecutive ISIs [48]. Research in spike timing has since focused on the inter-spike interval distribution [49] or the correlation between successive spikes. Analysis of the timing between spikes has discovered that the joint ISI histogram

of lags up to 6 ISIs in the p-type afferents behavior have a distribution that is partially described by a first-order Markov model and has suggested that neurons have a memory component with negative correlations, that can facilitate the detection of weak signals [50]. Research into understanding the effects negative correlations have on the noise have since been theorized through analysis from the signal detection and information theory perspective [44] and neuron modeling with a LIF model and dynamic threshold [51] to produce such behavior. The idea of noise shaping has been proposed [52], arguing that sensory neurons can be tuned to a range of frequencies based on their dendritic morphology [53], [54]. Speculation on the ionic interactions responsible for this behavior had been associated with the impact on the threshold of a neuron's firing, with outward potassium currents and inactivation of sodium channels as possible mechanisms [55]–[59].

In terms of spike timing precision, one notable report had injected current stimuli in layer 5 cortical neurons and had recorded spike timing and found that neurons can be very precise in their firing under certain conditions. In this case, presentation of stimuli with noise mimicking synaptic effects had increased spike time precision and reliability across multiple trials [60]. Cortical spike times are reliable under certain conditions, and the sources of noise that have been responsible for the noise are channel noise (i.e., intrinsic noise) and effects from noise from the synapse. In an experimental and computational study in hippocampal CA1 neurons from postnatal day 5-7 rats, downregulation of delayed rectifier potassium channels decreases spike-time precision [61].

The research in the stochasticity of neural spike times have been approached in many ways. In any given area of the neuron, there are numerous ion channels of any given type. The Hodgkin-Huxley model views the behavior of ion channels in the same types as mean response. As the number grows large, its limit is the expression highlighted by equations above. More information is known now about the physics of ion channels since the formulation of the Hodgkin-Huxley [62]. The Hodgkin-Huxley equations treat the conductance for channels as a composite of numerous channels of a specific type. Fluctuations in a channel's conductance,

however, can arise due to a finite number of channels in a single neuron, and is termed channel noise. Numerically, the effect of individual channels to model neurons can be implemented as Markov-chain Monte Carlo (MCMC) simulations [63]–[65]. One consequence of MCMC models is the increase in computational cost as the numbers of individual ion channels increase. In practice, estimation techniques in ion channel noise were used instead to produce a stochastic biophysical model of neurons. [66]. One of the techniques scales noises into dynamic gating variables and is called the Langevin approach (Fox and Lu, 1994). However, debate in the accuracy of the Langevin approaches based on Hodgkin-Huxley equations emerged, citing inconsistency with behaviors modeled by MCMC models [67]–[69]. Modifications to the Langevin approaches, such as introducing colored noise, dynamic conductance, and generalizing the form of the Hodgkin-Huxley, however, have since improved accuracy [66], [70], [71]. The study of noise in neurons has conjectured possible utility for exhibiting such behavior. Stochastic resonance has been coined in the field, adopted from its physics term. Stochastic resonance is a phenomenon in nonlinear systems where noise improves signal transduction and detection in many physical systems. The term had been applied to neuroscience as a possible way to describe certain effects of noise in a single-neuron and population level. However, the term is now used less frequently, and discouraged, in favor of more specific descriptions [72]–[74].

2.3.1 Optimal Source Coding

Historically, the encoder and decoder mechanisms that neurons follow have been treated as events happening in separate neurons, typically arranged as pre-synaptic and post-synaptic neurons. In this motif, a neuron codes its input in a spike train and communicates it to a post-synaptic neuron which "decodes" the input by means of synaptic filtering. The idea behind neural source coding [11] is that the encoder-decoder mechanism is contained within a neuron. That is, a neuron encodes its input into a spike train, and then simultaneously decodes it so that it maintains a running estimate of the input. This estimate is fed back to a

comparator which calculates the ongoing coding error (the difference between the input and the estimate). The coding error is input to the spike generator. In the event where the error between the internal decoder and input stimulus exceeds a threshold, an action potential is generated. Thus, the neuron encodes the coding error [11]. The principle of coding the stimulus error is mathematically like optimal coding in digital systems and is called source coding or data compression [75]. In analogy with the digital scheme, Jones et al. [11] refer to the model neuron as a source coding neuron.

There are two key features of the source coding neuron. The first is the internal estimate of the input via linear filtering of the spike train. In the simplest form the linear filter is a simple lowpass filter (a first or second order lowpass filter). The second is the comparison of the estimate with the input to generate a spike when the error reaches a preset threshold. When both are taken together, the estimation filter emerges as the well-known dynamic threshold [35]. The theory of a source coding neuron supports the idea of a dynamic threshold, where the tendency to fire successive spikes rapidly is resisted by the neuron in the form of increased refractoriness and causes firing rate adaptation. That is, the time to next spike is based on the history of previous spike times. Jones et al. [11] hypothesize that a voltage-gated potassium channel (the M-channel, Kv7/KCNQ) forms the basis for adaptation in a source coding neuron, and more specifically, the M-channel is responsible for the optimal timing of spikes so that the coding error is minimized for a given long-term spike rate.

2.3.2 M (muscarinic) current

M-current refers to a non-activating voltage-gated potassium current elicited by channels formed from the Kv7.2/7.3 (KCNQ2/3) family and characterized by its slow non-inactivating kinetics. The channel of this current is formed as a tetramer of Kv7.2 and Kv7.3 subunits in neurons. The excitability of this channel is well known, with disorder of the M current being implicated in pathologies such as epilepsy. The M-current was named for its observed effect of increasing neuron firing during the presence of muscarine [13]. The mechanism of

the increased firing is a muscarine-bound receptor which blocks the M-current. In addition to muscarine, channels associated with the M-current are affected by regulatory molecules such as calmodulin and phosphatidylinositol-(4,5)-bisphosphate (PIP2), which plays a metabolic role of regulation of the channel [76]. The precise mechanism of how Kv7 channels are regulated from such molecules remains an active study in research [77], [78]. The aim of this thesis relates M-current to regulation of spike timing.

The M-current channels (KCNQ/Kv7) are colocalized with voltage-gated sodium channels in the axonal hillock by ankyrin-G [79], [80]. Ankyrin-G (or ankyrin-3, ANK-3) is a cytoskeleton scaffolding protein found in the axonal initial segment (AIS), the site of the axonal hillock [81]. Within the AIS, the expression of Kv7.2 (KCNQ2) and Kv7.3 (KCNQ3) subunits is highest at the distal portion of the axonal initial segment [21], [82]. The localization of Kv7.2/7.3 in the AIS and its slow activation dynamics leads us to hypothesize that the M-current has a crucial role in spike timing.

2.4 Summary

Encoding models can be phenomenological, biophysical, or somewhere in between. Work in phenomenological threshold models has been successful in predicting spike-timing in neurons [1], [83]. The understanding of thresholds in neurons has been viewed as mathematical abstraction since a neuron's response is stimulus dependent. The concept of a threshold has nevertheless been useful in understanding neural coding at the single neuron level. It has led to insights relating signal detection and information theory into the types of behavior seen in spike timing statistics. This thesis is inspired by work from Jones 'and colleagues' [10], [11] derivation of optimal source coding in neurons. The aim is to produce a biophysically plausible neuron model that accurately predicts spike timing and jitter in experimental data. I implement a minimum channel Hodgkin Huxley-type model fitted to a publicly available dataset [2] in rat layer 5 cortical pyramidal cells to reproduce firing behavior.

Chapter 3

A Slow Activating Outward Current (M-Current) is the Dynamic Threshold of Neurons

3.1 Introduction

In the sensory system, information about the world around us is transmitted through neurons as a sequence of spikes. The information carried through these spikes conveys information about the stimulus, or features of it. The investigation in the neural encoding of this information has produced evidence of various types of coding mechanisms, from the early theories of rate-coding and spike-time coding to more specialized cases. With an ever-growing amount of discovery revealing the complexity of neural composition, neural architecture and chemical milieu, the modeling of neuron behavior becomes ever more difficult. One of the earliest biophysical models of neuron firing behavior is the Hodgkin Huxley neuron [29]. The Hodgkin Huxley considers Sodium, Potassium, and leak channels and produces a relation between the ionic gradient and spiking of a giant squid axon. Sensory neurons have been shown to fire in a consistent manner according to their input stimuli [60] and

voltage-gated ion channels are known to play a role in this precision [84]. In addition, the idea of a spike threshold of a neuron has been thought to be dependent on a membrane time constant, with "both the magnitude and the rate of V_m depolarization" [85], [86] being responsible for the change in threshold following the history of spikes. Spiking models have been developed to replicate the spiking behavior of neurons. In terms of spike timing, one of the best performers of replicating spiking behavior is the MAT model [1]. The MAT model is a purely mathematical model that explicitly incorporates an adaptive threshold, with parameters believed to be formed by outward potassium channels [87].

One of the most well-known channel models is the Hodgkin-Huxley type model; however, precision in spike timing has not been directly demonstrated in a Hodgkin-Huxley model. The goal of this paper is to investigate the individual ion currents from a model and validate by fitting real data. The first result of this work shows that a single-compartment, Hodgkin-Huxley-type model is not only capable of fitting a neuron's timing response, but also to introduce a single-compartment model with four voltage-gated ion channels that attains the best prediction of any published model of spike times for Layer 5 pyramidal neurons. This "minimum" model aims to minimize the number of voltage-gated ion channels possible in a Hodgkin Huxley model while maintaining spike-timing precision. These include Hodgkin Huxley channels (Na_T, K_{DR}, and Leak), Persistent Sodium (Na_P), Muscarinic Potassium Current (K_M). Channels in the model are modeled from channels known to exist in the spike initiation zone (e.g. Axonal Initial Segment or AIS). It produces the most accurate model to date, in terms of capturing subthreshold membrane voltage and spike times. Another advantage of this model is that it is more physiologically grounded than abstract mathematical models [1] and allows us to probe the voltage-gated ion channels that comprise it, providing insight into the physiological mechanisms by which neurons produce adaptive threshold behavior. We use the minimum Hodgkin-Huxley type model to investigate the influence of individual ion currents on short-term adaptation or an adaptive threshold and show evidence supporting the role of the M-type Potassium current in the adaptive threshold.

3.2 Methods

3.2.1 Neuron data

The dataset used here was obtained from a publicly available source, The 2009 INCF Spike Time Prediction Competition organized by the International Neuroinformatics Coordinating Facility (INCF). The competition provided datasets with a challenge to reproduce the spike-times using any computational model. The results of the competition are summarized by Gerstner and Naud (2009). The data set from one of the four challenges (Challenge A) is considered here and consists of *in-vitro* current-clamp recordings from a Layer 5 pyramidal cell in the rat somatosensory cortex. The data includes the neuron's response (intracellular membrane potential) to 13 repeated trials of frozen noise mimicking post-synaptic currents, of 21.5 s duration. The average firing rate of the neuron is about 10 spikes/s. The injected current and membrane voltage were sampled digitally at 10 kSamples/s. The data set includes an initial portion with response to step currents, but it is not considered here. The data are available in the public-domain along with a complete description of the methods from the organizers[1].

3.2.2 Model

The goal of the study is to model and predict the membrane voltage of the pyramidal neuron in response to a stimulus and infer intrinsic properties that could point to mechanisms of spike timing. The model used here is a classical Hodgkin-Huxley (HH) neuron [29], [88] with two additional voltage-gated channels. The classical HH neuron models action potentials at the Node of Ranvier of a squid giant axon and is a spike generator consisting of a voltage-gated sodium channel (Na_T), a voltage-gated potassium channel (K_DR), and a leak channel (L). The voltage-gated activation of NaT and KDR are relatively fast with the K_DR being delayed

[1]Dataset currently managed by the Collaborative Research in Computational Neuroscience https://crcns.org/data-sets/challenges/ch-epfl-2009. Contains current stimulation protocol of frozen noise for 35 seconds, but first 21.5 seconds are available to public

relative to that of the Na_T current. These currents produce the stereotypical shape of the action potential, with the KDR contributing additionally to a refractory period. We are interested in the axonal hillock where spikes are initiated from a generator potential that consists of the summated input arising in the dendrites and soma. This region of spike initiation is central to encoding because it produces a sequence of timed impulses in response to the input. Our hypothesis is that memory or history effects in the evolution of the membrane voltage, particularly with respect to timing of action potentials, requires relatively long-duration conductances which span one or more interspike intervals. Such memory cannot be due to HH conductances. Thus, in addition to the "fast" voltage-dependent HH conductances, we add two slow and relatively long-duration (i.e., non-inactivating) currents from a potassium channel (K_M, or M-channel) and a sodium channel (Na_P, or persistent sodium). We hypothesize that the M-current substantially accounts for the timing of action potentials, whereas the persistent sodium current is necessary to maintain a plateau potential (described in the Results) but is not involved in the timing of action potentials. All these channels are found in the axonal hillock in the spike-initiating region [22], [23], [89]. The goal here is to estimate the parameters of these five channels or conductances so that the model neuron reproduces the membrane potential from the experimental neuron. More specifically it must reproduce the timing of the observed action potentials.

The parameters are obtained through a fitting procedure described for varying numbers/types of voltage-gated ion channels. One major change was that the conductance-based model differs from the model previously described by Meliza and colleagues' [16] by including only voltage-gated Sodium Channels and Potassium Channels. The range of parameters in the fit were selected to have the nonlinear equations resemble channels seen in Layer 5 rat pyramidal cells (Appendix, A1). The lumped conductance-based model for the five channels

reported in this work are described by the following equation for membrane voltage:

$$\begin{aligned} C\frac{dV}{dt} = &- g_{NaT}(t)(V - E_{Na}) - g_{Kdr}(t)(V - E_K) - g_L(V - E_L) \\ &- g_{NaP}(t)(V - E_{Na}) - g_{KM}(t)(V - E_K) + \frac{I_{Input}}{I_{scale}}, \end{aligned}$$

where V is the membrane voltage, E_i are the reversal potentials for the ions $Na^+$and K^+, and the leak channel L, and g_x are ionic conductances for the five channels. I_{input} is the injected current and I_{scale} is a scaling term related to the compartment size. The first three ionic currents in the above equation correspond to the spike-generator, i.e., they are the classical Hodgkin-Huxley conductances, whereas the next two ionic currents are assumed to be specific to the axonal initial segment. The leak conductance g_L is constant and lumps the contribution from passive $Na^+$and K^+ channels. The conductances for the four voltage-gated ion channels are time-varying and voltage-dependent as follows: i) The fast conductances g_{NaT} and g_{Kdr} are time- and voltage-dependent and take the form $g_x = \bar{g}_x m_x^a h_x$ where x refers to the conductance, $\bar{g}_x$ is the maximum mean conductance, m_x is a time-varying activation, and h_x a time-varying inactivation. The parameter a is an integer exponent with $a = 3$ (Na_T) and $a = 4$ (K_{DR}). ii) The slow conductances g_{NaP} and g_{KM} have a time-varying activation (m_x) gate but no inactivation gate and are of the form $g_x = \bar{g}_x m_x$. The gate equations for m_x are of the form

$$\frac{dm_x}{dt} = \alpha_{m_x}(V)(1 - m_x) + \beta_{m_x}(V)\, m_x.$$

The equation for h_x are of the same form. The voltage-dependent parameters, α and β, are specific for each voltage-dependent conductance (see Appendix for the full expressions). There are a total of 41 undetermined free parameters in the voltage and gating equations: i) The current equation has 10 free parameters which include capacitance C, scale I_{scale}, reversal potentials E_{Na}, E_K, and E_L, leak conductance g_L, and max conductances $\bar{g}_{NaT}$, $\bar{g}_{Kdr}$, $\bar{g}_{NaP}$, $\bar{g}_{KM}$. ii) Each gate equation has 5 free parameters (see Appendix), and therefore 6 gate

equations result in 30 free parameters. These are the parameters to be determined so that the membrane voltage predicted by the model matches the experimental data. During model fitting, these parameters are constrained so that they take values within a physiological range [12], [15], [22].

3.2.3 Parameter estimation

The parameter estimation procedure is based on the interior-point optimization (IPOPT) implementation for nonlinear programming [90] with some modifications by Toth and colleagues [91], Kostuk et al. [92], Meliza et al. [16], and Nogaret et al. [14]. Parameter optimization follows the procedure described by Meliza et al [16] using IPOPT and the IBM Watson Sparse Matrix Package [93]. The model was fit for the first two seconds of the membrane potential response to noise input (see Methods). The fit parameters were then used to predict the membrane potential for the remainder of the noise input for all 13 trials. The cost function to minimize during optimization was the mean-squared error between the predicted and recorded membrane voltage, i.e., if the recorded membrane voltage is $y(t)$, and the predicted model voltage is $\hat{y}(t)$, then in discrete-time, we minimize $\sum_n (y[n] - y[n])^2$. Next, the data that were not used for the fitting (about 19-20 seconds) were evaluated for all 13 trials, and the average coincidence metric was obtained. A coincidence metric for the trial with the optimized fit was also recorded.

3.2.4 Analysis

The remaining segments of the INCF dataset not previously included in the fitting process were predicted by the model and compared to the neural response of real data using a spike coincidence metric [94]. The coincidence factor was used as a comparison between the neural recording and the response of the neuron model to the injected current.

The dynamic I-V curve [31], [32] measures the mean transmembrane current at different sections of the action potential. Traditionally, the I-V curve is obtained experimentally

through voltage-clamp preparations. The dynamic I-V curve provides a way to estimate the current-voltage relationship and serves as a tool to compare models to experimental current-clamp data. In addition, the dynamic I-V curve can estimate spike thresholds within given pre-spike and post-spike time windows (i.e., 5-10 ms, 10-20 ms). We obtain the dynamic I-V curve to estimate the time course of an adapting or dynamic threshold.

Evaluation of model for biophysical plausibility

To verify that the optimized fits to the channel parameters are physiologically plausible, we compare the voltage-dependent gating probabilities and time-constants obtained from voltage-clamp simulations with values determined for Layer 5 pyramidal neurons (see, for example, [17]. The goal here was to verify that the parameters were within the range of values normally encountered in the literature.

Detect presence of adaptation

The post-spike Dynamic I-V curve during different time segments shows the estimated spike threshold. The spike threshold for the model and INCF membrane potentials are estimated in the following time segments (post-spike): 5-10 ms, 10-20 ms, 20-30 ms, 30-50 ms. The responses of Hodgkin-Huxley type models are deterministic and do not change over repeated trials. To produce a peri-stimulus time histogram (PSTH) which includes variability in the response, the model was evaluated for a deterministic step input with additive noise. Noise power was low compared to the DC value of the step. The PSTH responses are useful for several reasons: 1) they provide an estimate of the Dynamic I-V curve, 2) the progressive decorrelation of the spike train over time in response to current steps can be observed, and 3) rate-intensity curves can be obtained (spike rate versus DC current input). All these measures can be obtained for the model neuron; however, only Dynamic I-V curves can be obtained from the INCF recordings. No PSTH data were available for the pyramidal neuron.

Effect of ion channel conductivity on spike firing rate

Voltage-gated Potassium channels have a strong effect on spike firing rate because they generate outward current which tends to make the neuron more refractory. We tested the hypothesis that the M-channel (K_M) modulates spike firing rate in inverse proportion to total average conductance, but the conductance due to the delayed rectifier (K_{DR}) has limited influence on the firing rate. We vary the maximum conductances g_{KM} and g_{Kdr} estimated from parameter fitting (considered to be 100% or nominal value) from 50% to 130% of the nominal value and obtain the mean firing rate in response to a fixed current input.

3.3 Results

Our goal was to obtain the best fit to the membrane potential of an experimental layer 5 pyramidal neuron with the smallest number of voltage-gated channels in a single-compartment model. The rationale is that we are interested in the axonal initial segment where a spike is initiated, and we argue that in this region, a single compartment will suffice. We began with the classical Hodgkin-Huxley model (Na_T (transient sodium), K_{DR} (delayed rectifier potassium), and L (leak) channels) and attempted to hand-tune the model to fit the membrane potential to the experimental data. The initial results were poor in matching spike timing (data not shown). This is not surprising, because the classical Hodgkin Huxley equations model the action potential recorded from the node of Ranvier in the giant squid axon, which acts as a repeater. We added two slowly activating channels, a persistent sodium channel (Na_P) which captures the plateau potential seen in the experimental data, and an M-current (K_M) to regulate spike timing. It should be noted that the persistent sodium current due to the Na_P is not necessary if the plateau potential is not present. The only modification we made was to the delayed rectifier K_{DR}, where we added an inactivation gate. The KDR in the classical Hodgkin-Huxley model included only an activation gate. We will discuss this in detail later. The parameters of the model were fit using an interior-point-optimization

procedure [16], with multiple unique fitting sessions to find a set of parameters that minimized the mean-squared error between the membrane voltage generated by the model, and data from the INCF pyramidal neuron.

3.3.1 A minimum model of a single compartment model describes spiking behavior seen in a layer 5 pyramidal neuron

With the two criteria of spike-time precision and minimum-mean square voltage error, the parameters we present are likely suboptimal since interior point optimization results in a locally optimal solution, but well enough to make some claims about biophysical ionic conductance. We first look at qualitative aspects of membrane voltage in response to current injection. In the training set, 2 seconds of data were used. In the test set, the 2 seconds of data were included with 19.5 seconds of stimulus following the original 2 seconds. In total, 21.5 seconds from both the training set and test set were predicted from the model and compared to the neural recordings (Fig. 3.1).

Comparison between the voltage trace of the model and INCF show a reasonably good fit. Insets a and b in Fig. 3.1A demonstrate that the model occasionally adds a spike. Other segments sometimes show deleted spikes. However, the figure demonstrates that the relatively simple conductance model can reproduce spike times fairly accurately despite the model being deterministic. A phase plot was used to explore the change in the voltage over the duration of the spiking events (Fig 3.1A) but did not prove meaningful in the context of spike-time precision. The model and experimental data have similar rise characteristics (Fig. 3.1B), but differ in their repolarization phase, with the model repolarizing more rapidly than the experimental neuron. Comparison between the voltage trace of the model and INCF show a reasonably good fit

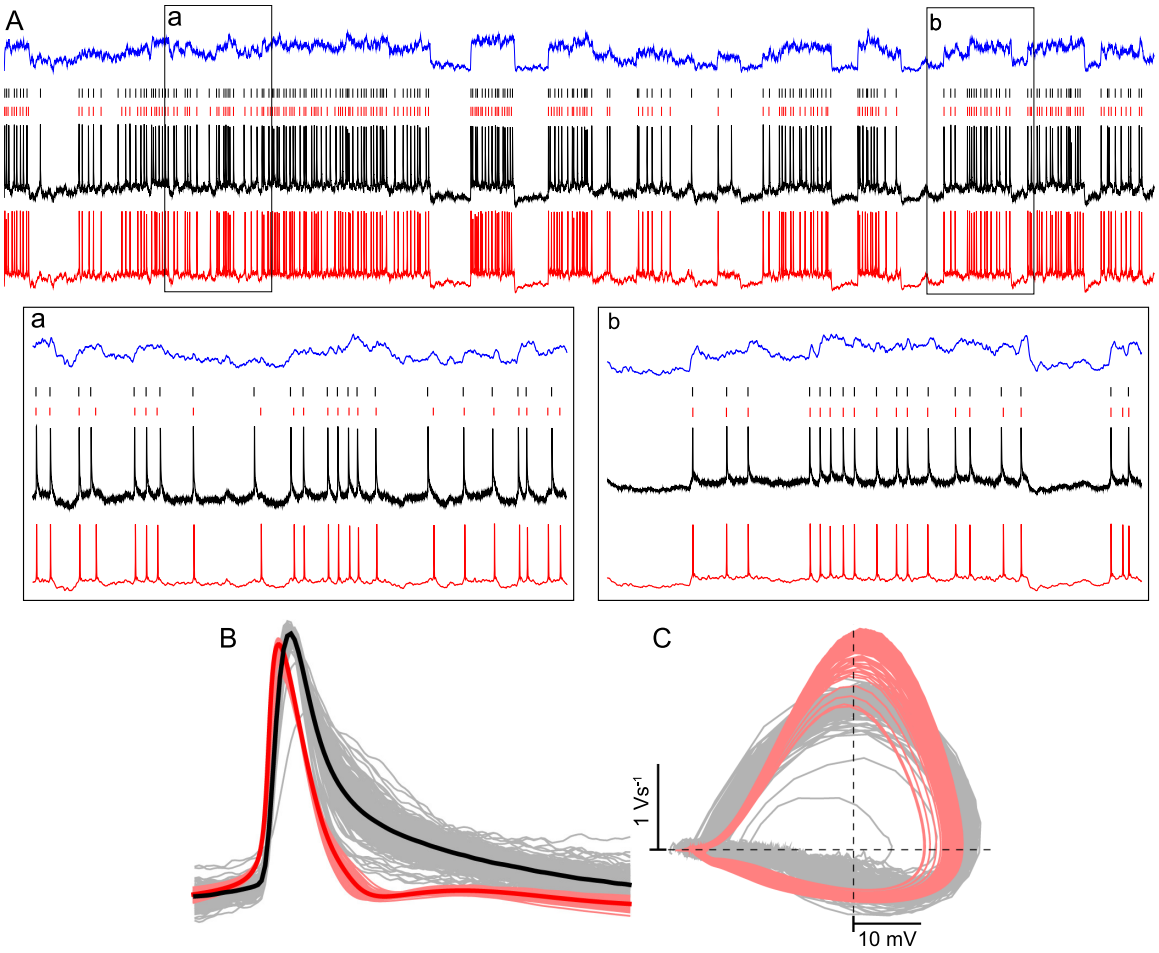

Figure 3.1: Comparison between the membrane voltage of the minimum Hodgkin Huxley model (red) and recorded data (black): a) an example trace of ∼2 seconds of data overlaid with model prediction, above shows a raster of the corresponding data. B) voltage potential for a single spike and average for the model (red) and data (black). C) Phase response for model and data.

3.3.2 Spike-time precision as measured by a coincidence metric shows reasonable accuracy

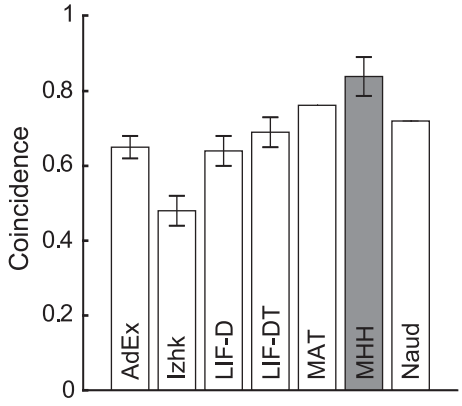

Figure 3.2: Comparison of spike time coincidence between models and the INCF pyramidal neuron data. The minimum Hodgkin-Huxley based model (MMH) is shown as a solid grey bar with normalized coincidence factor (Γ_A) 0.84. Other models (arranged in random order, with coincidence factor in parenthesis) are the adaptive exponential integrate-and-fire (AdEx) model (0.65), Izhikevich (Izhk) model (0.48), adaptive leaky integrate-and-fire (LIF-D) model (0.64), leaky integrate-and-fire with dynamic threshold (LIF-DT) model (0.69), multi-timescale adaptive threshold (MAT) model (0.76), and the Naud model (0.72). Data for AdEx, Izhk, LIF-D, LIF-DT are taken from Rossant et al. (2014), the MAT model from Kobayashi et al. (2009), and Naud model from Naud et al. (2014). Standard error is shown where available.

We obtained the spike time coincidence measure between the predicted spike times from our model and the actual spike times (Fig. 3.2, MHH), and further, compared the timing coincidence with other models that used the same INCF data set for prediction (Fig. 2, see caption for model descriptions). Our model captures timing accuracy in about 84% of the spikes (and provides the best spike timing accuracy among all the models evaluated with the INCF data, so far). The winning model in the 2009 INCF Spike Time Prediction Challenge was the multiadaptive threshold model (MAT, [1]) with a relative coincidence, Γ_A =0.76 (see also [95]). The remaining models (see Fig. 2, and [96]; [97]) demonstrate lower spike time coincidence. The only Hodgkin-Huxley type model (i.e., with biophysical conductances) is the MHH model, the remaining models are without conductances, with varying degrees of biophysical plausibility.

3.3.3 Estimating the I-V relationship using a Dynamic I-V estimate

To explore the model more analytically, we estimate the membrane-current relationship between the model and experimental data. Traditionally, the current-voltage (I-V) relationship is obtained from voltage-clamp measurements. This data was not provided by the organizers of the INCF challenge, and so we estimate the I-V curve using the dynamic I-V curve [31]. The dynamic I-V curve of the model and INCF data are estimated at four time-bins (5-10 ms, 10-20 ms, 20-30 ms, and 30-50 ms), postspike, where each bin is a time window with at most one succeeding spike. The dynamic IV curve uses the average of the membrane potential traces. The black, dashed line (Fig. 3.3) represents the "pre-spike" I-V relationship and is measured in a post-spike time window long after the spike (here 200 ms) so that the I-V curve has returned to its normative value. The pre-spike dynamic I-V curve is compared to the dynamic I-V curve for each respective time bin and shows regions of the model that fit the experimental data well, and those that do not. The region around spike initiation is within 4 mV of each other across the regions that spike. One useful piece of information we can obtain is the spike threshold for spikes that occur in each time range, indicated by the point at which the dynamic I-V curve crosses zero during the curve's rise (i.e., on the positive slope, Fig. 3.3A, 3.3B).

Due to the limited amount of data from the experimental recordings, the zero threshold can only be obtained by linear interpolation between the point below and point above zero. By comparison, the model data was simulated for the experimental current, and with much longer duration (100 minutes), with noise matching the power of the experimental current. This allows us to obtain a more accurate estimate of spike threshold (seen later).

One issue to point out is the inaccuracy of the model in the region from -50 to -65 mV. It appears to be heavily influenced by the sharp hyperpolarization of the Potassium delayed rectifier before rising again with the persistent Sodium current within 5 ms after the initial spike. With the model being restricted to the minimum number of channels in the axonal

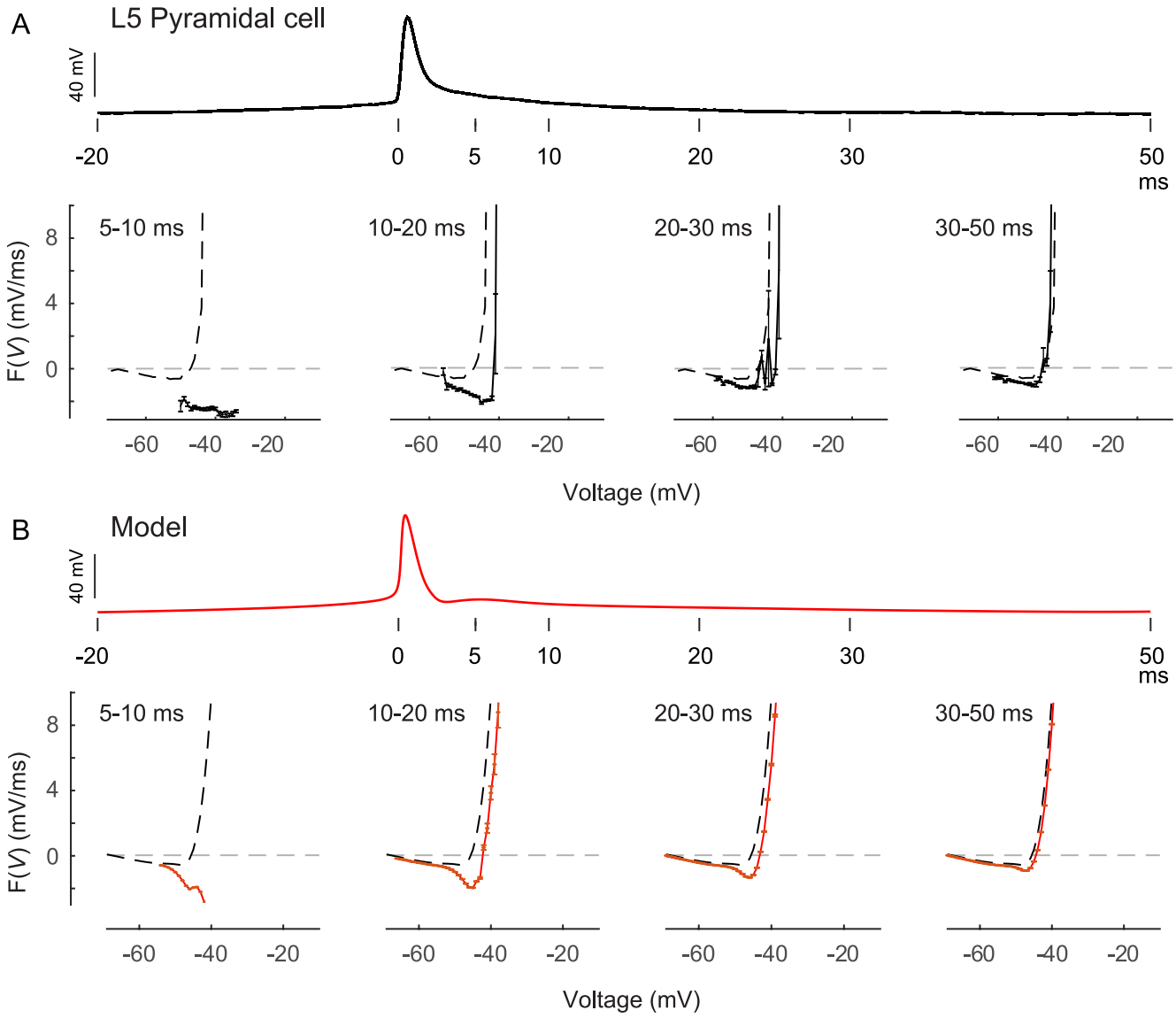

Figure 3.3: Comparison between the spike-time averaged trace between model (red) and experimental data (black) and their respective dynamic IV curve. Shown for post-spike dynamic IV curves within the range of 10 and 50 ms

hillock, and tuned to precisely predict spike timing, the model will not match the dynamic IV curve at every region. Since we are interested mainly in determining spike threshold and the timing of spikes, the minimum Hodgkin-Huxley type model is sufficient in our case.

3.3.4 Presence of an adaptive threshold exists as an outward Potassium current (M-current)

Previous researchers have shown that outward Potassium currents serve as regulators of spike-frequency adaptation [98]. Previous studies have shown that the parameters of an adaptive threshold model can be described by Potassium currents in a Hodgkin-Huxley type neuron [99]. However, we ask whether it is possible to construct a Hodgkin-Huxley type neuron, with the fewest number of ionic channels found in the axonal hillock, while precisely predicting spike times as in experimental data. The dynamic IV curve, as shown previously, allowed us to estimate the spike threshold at various time ranges. Using this approach, we calculated the threshold (from the dynamic I-V curve) for our model in 1 mV time bins for 100 minutes of simulated noise current, matched in power to the experimental current injection stimuli. We use this to demonstrate an adaptive threshold in the Layer 5 pyramidal cell. Figure 3.4 shows that for the Layer 5 pyramidal neuron, a dynamic, adapting spike threshold is likely to be present (black filled circles). A double-exponential fit, like that described by the MAT model [1], specified by $A_1 e^{-t/\tau_1} + A_2 e^{-t/\tau_2} + C$ gives $A_1 = 32.5$ mV, $\tau_1 = 9.00$ ms, $A_2 = 3.12$ mV, $\tau_2 = 105.5$ ms, and C=-44.2 mV demonstrates a fast exponential decay of 9 ms and a slower exponential decay at around 106 ms. This finding supports the idea of a dynamic (adaptive) spike threshold.

3.3.5 An adaptive threshold regulates spike firing

To investigate the role that individual ionic currents have on the behavior of the membrane potential after a spike, the normalized spike-triggered ionic current is used (Fig. 3.5). For

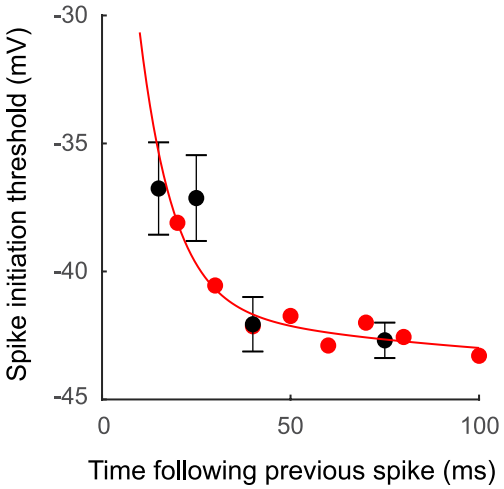

Figure 3.4: Threshold (mV) vs time (ms) of the model after spike for experimental pyramidal neuron (black filled circles) and our biophysical model neuron (red filled circles). A double exponential fit of the threshold for the model is shown in red. The fit is described by a fast exponential with time constant of about 9 ms, and a slow exponential with a time constant of about 106 ms. Parameters for the threshold fit are fully described in the text.

any given ion channel, each trace is divided by the norm of the trace between a -20 ms and 50 ms window about the spike. The M-current shows a noticeable elevation above baseline immediately after the spike as it slowly decays throughout the plot and continues for about 1.5 s (not shown). Other channels do not show such large excursions for a long duration. The leak current (Fig. 3.5) also demonstrates large amplitudes, but it is not sustained beyond 30-40 ms, sufficient for the membrane potential to return to rest. Both the M and the leak currents demonstrate a sustained outward current immediately following the spike threshold (i.e., the rising depolarizing phase) with the M-current remaining elevated for a longer duration. The leak current demonstrates less variability across spikes than the M-current. The larger variability in the M-current is due to the increase in ionic current from the history of spikes, i.e., the memory of the previous spike, and this presumably raises the threshold of the next spike. The smaller variability in the leak current is attributed to the fact that the leak current is an ohmic current, where the ionic contribution is directly related to the change in membrane potential. For the M-current and leak current, the associated time constants to a decaying exponential are 140 and 59.6 ms, respectively.

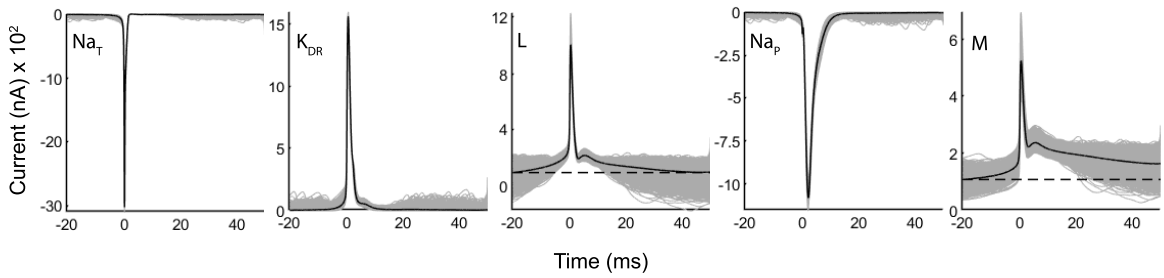

Figure 3.5: Spike-triggered ionic currents. Total response for each ion channel, overlaid to a fixed spiking event. The mean response for each ion channel is shown in bold. Dashed line indicates the baseline conductance prior to spiking event.

3.3.6 The peristimulus time histogram and regulation of firing rate

Adaptation to a sustained stimulus can be seen in the peristimulus time histogram (PSTH) depicted in Fig. 3.6A. A DC current step (550 pA) is presented repeatedly to the model neuron. To introduce noise in spike timing (and in the PSTH) low-power noise is added to the DC current (see red trace in Fig. 3.6A). For a sustained step current, the model neuron adapts its firing rate over time. Similar data is not available for the experimental data. The PSTH demonstrates the two timescales of adaptation reported in Fig. 3.4, namely, a rapid initial decline in firing rate, followed by a slower decline in firing rate until a plateau is reached.

We next looked at the effect of change in maximum conductance on the spike firing rate for the delayed rectifier ($\bar{g}_{Kdr}$) and the M-current ($\bar{g}_M$). Our hypothesis, based on the known properties of the M-current, is that the M-current regulates the baseline level of activity for a given bias input, by regulating spike timing. On the other hand, the delayed rectifier is part of the action potential generator (i.e., the impulse generator) and has no role in regulation of baseline levels of firing rate. We assume that the baseline firing rate is governed by the expression levels of the voltage-gated potassium channels, i.e., the mean channel density regulates the firing rate (see [22]). Consequently, the maximum conductance $\bar{g}_{Kdr}$ and $\bar{g}_M$ are surrogates for the channel densities, and their variations should cause changes in the mean

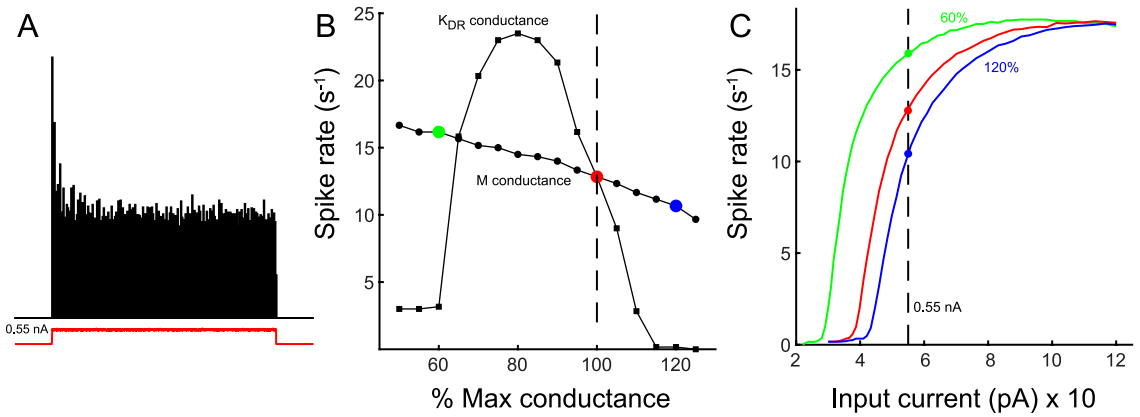

Figure 3.6: A) PSTH of our model neuron to a 550 pA DC stimulus. Low-power noise is added to the step current to cause variability in spike timing. 6 seconds of step current is used, with a 1 second gap in the start of the simulation, and 1 second gap at the end of the stimulus. B) Average firing rate vs percent maximum conductance of the M-current and the delayed rectifier potassium channels. Note that firing rate for the M-channel decreases monotonically with increase in total (max) conductance, whereas firing rate for the delayed rectifier is non-monotonic, dropping sharply from a peak firing rate at about 80% maximum conductance. C) Rate-intensity function parameterized by the maximum conductance of M-channel. Note the rightward shift in the rate-intensity function, indicating adaptation as the conductance changes from 60% (green), to 100% (red or nominal), to 120% (blue).

firing rate. We use the optimized values of the parameters for our model and denote the values of $\bar{g}_{Kdr}$ and $\bar{g}_M$ as the "nominal" or 100% values. We then scale these conductances from 50% to 125% of the nominal values (i.e., we effectively adjust channel density) and calculate the mean firing rate in response to a DC step current of 550 pA (as shown in Fig. 3.6A). The results are depicted in Fig. 6B. The M-current and delayed rectifier are outward potassium currents, and so we expect an increase in maximum conductance to decrease the average firing rate. However, the change in firing rate is non-monotonic for the delayed rectifier (square symbols) whereas for the M-current, there is a monotonic and proportional change in firing rate with the mean conductance (filled circles).

The adaptation of firing rate to stimulus intensity by the M-channel can be seen in Fig. 3.6C which depicts the rate-intensity function at three different mean conductance values: 60% (green), 100% (red), and 120% (blue). As the total (mean) conductance of the M-channel increases, the rate-intensity function shifts to the right, as expected, making the neuron more

refractory.

3.4 Discussion

Evaluation of the activity of model neurons by use of computational models suffers the tradeoff between biophysical realism and computational efficiency. Increasing complexity in a biophysical model, such as inclusion of a neuron's morphology, results in an exceptionally demanding task in fitting the membrane voltage produced by the neurons, with an extensive number of free parameters that will exponentially increase in the parameter space. Such massive models are computationally complex and require high-performance computing resources which make routine evaluation of models difficult. Thus, the model complexity must be reduced to allow reasonable parameter estimation times even in a high-performance computer. Biophysical models typically reduce the computational demand by fixing channel kinetics and limiting the fits to a handful of features of spiking activity instead of the membrane voltage itself. In addition, the difficulty in fitting a neuron model with extensive biophysical realism suffers the cost of interpretability of the model's mechanism. While there is a utility in using these multi-compartment models for studying neuronal population and meso-scale structures of the brain, this work aims to accomplish another objective. In Gerstner and Naud [95], it is mentioned that not much is known about the performance of biophysical models in terms of spike time prediction of experimental data, as in the 2009 INCF Spike Time Prediction Challenge. We argue the necessity, in our case, for utilizing a single-compartment biophysical model to describe the ionic channel behavior in real neurons. With the reduction of the model complexity, i.e., numbers of channels, a parsimonious model requires less data for fitting, and the extent of overfitting is decreased to the number of free parameters in an underdetermined system. Here, a single-compartment Hodgkin-Huxley type model is considered for this experiment, with only ion channels found in the axon initial segment. The methods used to fit a Hodgkin-Huxley type model to predict membrane voltage activity have

been successfully demonstrated [14], [16], [100] in zebra finch and mice neurons. We attempt to create a biophysical model that not only produces reliable spike-timing in rodent neurons, but we also investigate the impact of voltage-gated ion channels in short-term adaptation. Further, to narrow our search for probing into the effect of ion channels in adaptation, we first want to test the hypothesis of fitting a Hodgkin Huxley-type model with the minimal number of ion channel types necessary to produce spiking activity. This model with the three classical Hodgkin-Huxley channels which make up the spike generator are complemented with a slowly activating M-current to determine spike times. Additionally, a slow persistent sodium channel captures the plateau potential but is not necessary for regulating spike timing. This model is adequate to capture 84% of the spike timing. To our knowledge this represents the best-known fit to spike-times of any model and is the only known model with biophysically realistic conductances (see [95]).

While we took care to produce a biophysical model with equations that closely represent the ion kinetics, we cannot rule out certain limitations of the model. First, the parameters representing Sodium channels with very fast kinetics, such as the inactivation time constant of Na_T, result in a very flat time constant in the model that does not fully agree with the kinetics seen *in-vitro*. Second, we cannot rule out the possibility that any missing ion channel is being "compensated" by channels that are in the model. Third, the exclusion of Calcium channels in the model removes the impact of potential calcium-activated Potassium channels in the axonal initial segment [22]. Nevertheless, this presence of this small (and restricted) set of 5 channel types agrees with known channel types in the axonal initial segment (see [15], [36]). It is known that voltage-gated ion currents are involved in adaptation. There has been a large amount of evidence showing that the currents involved are outward potassium currents [61], [87], [98], [101], [102] and inactivation of sodium [56], [86], [103], [104]. In addition, we know that information processing from spikes can incorporate spiking events from structures apart from the axonal hillock. In this study, we focus solely on signal processing in the axonal hillock to see whether the timing between spikes can be explained by spiking from

only the axonal hillock. The extent of this study shows a large extent of spike-fitting can indeed be explained by the 4 channels in a Hodgkin-Huxley model. Since the data we are working with are *in-vitro* recordings from the soma, there are limitations to the data we wish to fit. Because our model only contains channels within the axonal hillock, the spike waveform will not match completely. Figure 3.1 shows the incomplete match to the data. This study puts more focus on the timing between spikes and investigated the presence of a dynamic threshold in the individual ion currents. The results of this study show that none of the nonlinear parameters of any individual ion current matches the decaying threshold of the dynamic threshold, which could point to the fact that a combination of multiple ion channels shapes the dynamic threshold. We do, however, show the contribution each channel, such as the M-current, during the time course of the spiking event and on the firing rate.

The justification for including the muscarinic current in a minimal biophysical model is detailed in the extensive work from ion channels. Evolutionarily speaking, neurons have preserved their functional role across multiple species [98], which we argue as having a largely fundamental role in information processing. The details of muscarinic (or Kv7.2/7.3/KCNQ channels) currents have been investigated through a large body of in-vitro neural recordings. Notably, these types of channels are found in a variety of neuron types, including cortical pyramidal cells and sensory afferent neurons [105]. The role of muscarinic currents has been associated with spike frequency adaptation [98] and can serve as a means of optimizing a neuron's spike-timing based with respect to energy expenditure [106]. The parameters for this model were obtained from a single neuron. The data source is an L5 pyramidal cell, which adapts for only small-time scales (18-50 ms), thus we cannot fully say that the leak current does not contribute at all to adaptation with this model. The limitation in our conclusions can be restricted to the amount of data used for this analysis. We aim to extend the model to a larger set of data and neuron types to further investigate the role of a dynamic threshold. The phenomenon incorporated in this model can explain the adaptive behavior, and this study builds upon the established body of work.

Chapter 4

A Minimum Hodgkin-Huxley Stochastic Threshold Model Describes Experimental Data

4.1 Introduction

In Chapter 3, I have presented a biophysical model capable of matching spike times in the cortical Layer 5 pyramidal neurons and have shown that a dynamic threshold is implicitly contained in the model. The dynamic threshold, as shown from analysis of the dynamic I-V curve, explains the variability in the spike threshold observed in the experimental data. However, the variability in the model, a Hodgkin-Huxley type with a persistent sodium (Na_P) and M-current, is deterministic, and the model lacks a stochastic element; upon repeated trials of the same stimulus, the model will produce identical spike trains. *In vitro* current clamp recordings of cortical neurons, upon repeated stimulation of the same injected current produce variability in spike timing. In real neurons, this is far from the case. With the same stimuli, a noise current was repeatedly presented to the neuron 13 times (Fig. 4.1). This method of repeated stimulation with a single realization of a random noise signal (called

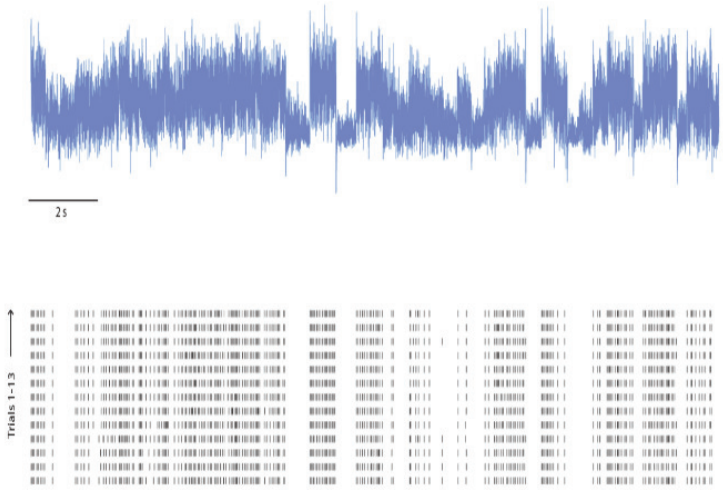

Figure 4.1: Raster plot of cortical pyramidal neuron response (INCF data set, see Methods). Upper panel shows injected noise current (blue trace) presented repeatedly (frozen noise), thirteen times. The lower panel shows the raster plot of trials (1 through 13). Action potentials are locked to features of the stimulus and spikes are generally reproducible. However, spikes are not perfectly aligned and exhibit some jitter. Additionally, some spikes may be added or deleted between trials.

"frozen noise") is referred to as a "frozen noise experiment". In the 13 trials of repeated stimulation with frozen noise, comparison of spike trains across trials shows that spikes occur with reliable timing in response to certain stimulus features with some timing jitter (Fig. 4.1). This allows us to identify a "coincidence" window for aligning spikes across trials. Given a small window size, spikes between trials found within the window are considered "coincident". However, not all trials may demonstrate coincident spikes. Thus, there are spikes which appear in some trials and but may not be present in other trials, i.e., spikes appear to be "added" or "deleted". This observation lends to the idea that such neurons are better described by a spike-timing code rather than a rate code [60].

Jitter in the spike timing suggests that there is a certain amount of randomness in the spike train. It does not alter the pattern of spikes seen in large scale, but on a smaller scale it will lead to small shifts in spike timing, or the deletion/addition of a spike. The aim of this research is to incorporate stochasticity into the model which has been fitted in

the earlier part of my research work, so that the model can accurately produce the timing jitter and the observed additions/deletions of spikes. Implications related to noise in the dynamic threshold, which is contained in the voltage-gated ion channels are explored. To recall, the Hodgkin-Huxley model is deterministic and does not produce variability in spike firing upon repeated trials. Since the equations in the Hodgkin-Huxley model calculate the average fraction of open channels rather than the summed contribution of individual ion channels, the output to a presented stimulus input is identical each time. One major, and noticeable difference in my modeling results is that my deterministic model can add an "extra" spike (re: the experimental spike train). This can be seen in Fig. 3.1A (insets a and b, see figure caption). It is not clear whether randomness can correct for the "extra" spikes and reproduce the random patterns as observed in the experimental data (with the same statistical properties in timing).

I will establish a stochastic extension of the previous model and predict both the timing jitter and the negative correlation between adjacent ISIs (see chapter 2 and [50]. The goal of this chapter is to provide a biophysically plausible source of noise that can be explained by the data and theory. Specifically, I will explore a noisy spike threshold to perturb spike timing. The method to introduce noise into the model described in Chapter 3 is fundamentally different from approaches in the literature [55], [63], [66], [71] in that it makes the maximum conductance of the M-channel stochastic but does so in a discrete way. Motivated by previous results obtained from colleagues [10], I introduce a stochastic biophysical model with noise in an adaptive current following each spike. I will compare the results of this model to experimental data through numerical simulation of repeated current injection stimulation, by analytical metrics of jitter. I will then compare the influence of increasing stimulus noise on jitter to the report of Mainen and Sejnowski [60]. and compare the effect of spike-to-spike correlated noise on the model to the theoretical derivation of Sidhu and colleagues [10].

4.2 Neuron Variability and Stochastic Models

The variability in trial-to-trial neuron firing is contributed to by numerous factors. The first, and most prominent, is noise due to network effects, i.e., caused by bombardment of synaptic input. The next are intrinsic effects: thermal noise and noise in the ion channels of the neuron. In vivo, extrinsic noise contributes to a large amount of variability, however, it is possible to control the network effects in an *in vitro* recording. Using current clamp techniques *in vitro*, Mainen and Sejnowski [60] have shown that a frozen noise stimulus produces per-trial reproducible spike timing within 1 ms jitter, whereas a constant step input does not, due to the accumulated effects of intrinsic noise over time. This suggests that the spike generation mechanism has a short integration time, where there is a level of intrinsic noise, or "channel noise" responsible for its variability that can be overcome when there is a high enough level of synaptic input[1].

The classical Hodgkin-Huxley equations represent the average opening and closing rate in a population of ion channels [29]. For a specific type of channel (e.g., K_{DR}, potassium delayed rectifier), the channels are lumped with each possible state (open, closed) and its transition to another state given as a probability which is the fraction of channels undergoing that state transition. Further, channels such as the fast, transient voltage-gated Na+ channel ($\mathrm{Na_T}$) have voltage-dependent activation and inactivation gates, each of which can transition between states. The gates are considered to operate independently and so their gating probabilities can be multiplied, as Hodgkin and Huxley [29] had done. There are methods to simulate stochasticity in Hodgkin-Huxley type models. One method treats the differential equations for the gating currents as stochastic differential equations by adding a scaled stochastic noise term to the dynamic gating variables. The noise term is a white noise process and is scaled based on the membrane voltage. Another method simulates opening and closing of individual ion channels with Markov Chain Monte Carlo (MCMC) simulations to calculate

[1] In Mainen and Sejnowki's research [60], noise in current stimuli was filtered before injection to represent excitatory/inhibitory post-synaptic potentials.

the membrane voltage. Since the opening and closing behavior of individual ion channels are probabilistic, their inherent stochasticity appears from the finite number of ion channels in the simulation.

The aim of this study is to replicate jitter seen in experimental data in a biophysically plausible way. In addition, a stochastic optimal coding model, where noise is introduced in the spike firing threshold, has been reported [10] which explained spike-time behavior in P-type electrosensory afferents in the weakly electric fish ([50]). In the biophysical model, the analogue to a threshold is not as clear. The equations in the Hodgkin Huxley model are non-linear and coupled to the membrane voltage. Thus, mathematical analysis in this system will be very challenging. In the literature, there are two competing ideas of the primary contributor to a dynamic threshold, those being the inactivation of the fast sodium channel (Na_T) or the M-current (K_M). Hence, careful consideration and a systematic approach in implementing stochasticity into the Hodgkin-Huxley model is explored. To what extent does noise in the ion channels contribute to jitter shown in experimental data? Are the spike timing statistics captured from such noise? Is it possible to show that the stochastic model is affecting the dynamic threshold?

4.3 Methods for Evaluation

Neuron variability has been measured by different methods, from either the physiologist or the modeler's perspective. In physiological experiments, the precision, reliability, Fano factor, and serial correlation coefficient metrics are used. Across the literature, there are many different approaches to measuring spike timing jitter [60], [94], [107]–[109]. A metric described by Bair & Koch [60], [109] considers the possibility of trials having deleted, added, or shifted spike times, called the precision metric. It does so by gathering the peristimulus time histogram (PSTH) of the trials and measuring the standard deviation of the peaks in the PSTH. Another metric, reliability, calculates the summed pairwise correlations of spikes

and considers the standard deviation of the largest peak as the measure of jitter.

In the Markov-chain modeling of ion channels, the four metrics are threshold, relative spread, spike latency and jitter [68], [110]. The threshold in this notion is the intensity of stimulus needed to produce a spike, and relative spread is measured as the coefficient of variation of the threshold. The following methods are used in the evaluation of the model: jitter and serial correlation coefficient.

4.3.1 Jitter

A metric of spike timing variability is generally measured as the jitter in spike-times between trials. The calculation of this measure depends on the stimulus and time scale. Across a large timescale, under constant stimuli, jitter can be calculated as the standard deviation of the difference in interspike intervals (ISIs). However, this results in a very coarse evaluation and does not provide fine information. The assumption underlying this calculation is that the noise in the system is gaussian. Further, the metric has dimensions of time which makes it difficult to compare across spike trains with differing mean spike rates.

In chapter 3, the coincidence metric Γ [94] was used to measure similarity in spike timing and measures the precision of spikes across various coincidence windows. We had used this metric in the previous section when evaluating the best fit in spike times. Here, we will modify the coincidence metric so that the effect of window duration does not impact the metric. The jitter will be calculated as a function of coincidence window duration, and normalized by the duration, so the jitter becomes a dimensionless quantity. The coincidence metric can be modified in a way to give a measure of spike timing jitter. If N_{coin} was decomposed into a set of spike times for all trials in a dataset, the difference within a coincident window between two trials can be calculated. Following normalization by the window size and number of coincident spike times, we can have a reasonable measure for jitter. The pairwise metrics of a given window can be summed to produce a single value that ranges from zero to 1, with zero showing perfect spike timing for all times (i.e., spike timing would be deterministic). The

formulation will then be:

$$\Gamma = \frac{\sum_{i<j}^{\text{ntrials}} \| [spiketimes\,(i) - \quad spiketimes\,(j)]_{coin} \|}{|N_{coin}|\,\Delta}$$

where $i, j \in \mathbb{I}^{+}$. For a set of trials, (in this case, the INCF dataset containing 13 trials), this modified form of the coincidence metric will be applied with coincidence values from 1-40 ms in 1 ms increments and plotted against window size. Similarly, the procedure is performed for the model simulation data of 13 repeated trials and overlaid on the same plot in order to compare regions where the similarities occur between the data and model.

4.3.2 Serial Correlation Coefficient

Serial correlation coefficients are measured as the correlation of inter-spike intervals between a given ISI and an ISI k lags apart [50], [111]. The ISI serial correlation coefficients (SCCs) have a characteristic behavior. For each pair of ISIs separated by lag k, the SCC is calculated as:

$$\rho_k = \frac{\sum_{i=1}^{M-k} \left(j_i - \overline{I_1}\right)\left(j_{i+1} - \overline{I_1}\right)}{\left(\sum_{i=1}^{M-k} \left(j_i - \overline{I_1}\right)^2 \sum_{i}^{M-l} \left(j_{i+1} - \overline{I_1}\right)^2\right)^{\frac{1}{2}}},\ l = 0,\ 1,\ \ldots\ ,$$

where I_1 is the mean ISI, M are the total number of successive ISIs, and $j_1, \ldots, j_M$ are the sequences of ISIs in M. The values of ρ_k are from -1 to 1, where positive numbers are positively correlated, and vice-versa. When estimated as a function of the ISI at lag k, the SCC at k = 1 (adjacent ISIs) for strongly negatively correlated spike trains is around -0.5, and then the magnitudes of the SCCs decay to zero with increasing lag.

4.4 Model Considerations

In implementing stochasticity into a biophysical model, a consideration of the literature on past implementations on Hodgkin-Huxley and voltage-gated ion channels is addressed. Three approaches in a stochastic biophysical model were considered: 1) introducing noise in

the activation gates, 2) modifying $V_{1/2}$, or 3) modifying a channel's maximum conductance. White [68] has described the inaccuracy of the Langevin approaches to the Hodgkin Huxley model compared to its equivalent MCMC form. However, Goldwyn et al. [66] have revisited Langevin method-based Hodgkin-Huxley models, where they re-implement the method originally formulated by Fox and Lu [112], where the Langevin form of the Hodgkin-Huxley equations were derived. Although the researchers have mathematically derived a Langevin solution directly from the Fokker-Planck equations of K_D and Na_T from Markov chains, they have not applied the approach to simulated data. Goldwyn found that "independent subunit" and "identical subunit" Stochastic Differential Equation (SDE) models, which retain the equations of Hodgkin and Huxley, are not mathematically equivalent to Fox and Lu's derivation. That is, a generalized form does not employ a Hodgkin-Huxley formalism, is its proper implementation [66], [70]. With Langevin approaches that retain the Hodgkin-Huxley equation, noise introduced in biophysical conductances, rather than the dynamic gating variables, improves accuracy to experimental data [71].

Studies have reported that inactivation of sodium is associated with the change in threshold [56], [103], [113]. Others claim an outward potassium current is involved [11], [57], [58], [87]. In effect, there is memory in the spike trains (see also [10], [50]). Since the distinction between an adaptive current and dynamic threshold is clear [3] (see background), the challenge is in introducing noise into a dynamic threshold that occurs indirectly through the change in the Hodgkin-Huxley model. However, *in vitro* slice preparations may not create variability in the inactivation of sodium due to loss of network effects and change in kinetics from *in vivo* conditions [103].

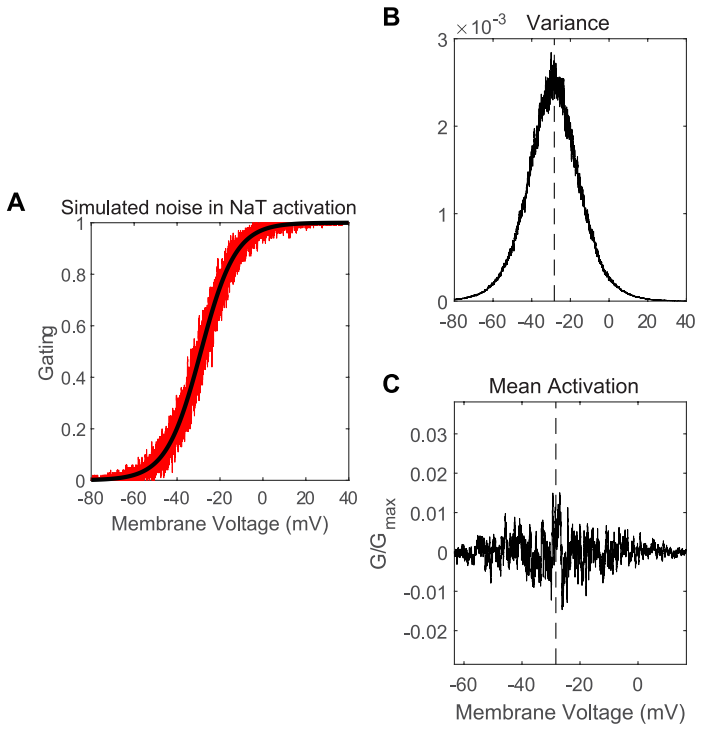

Figure 4.2: Randomness observed in a Markov-based ion channel model of the Na_T current. Simulation of 100 Markov-chain at 1000 trials. A: Activation of Na_T gating across a population of channels (individual traces are shown in red, average in black). B: Variance in the membrane voltage resulting from the A, the peak in the variance (dashed line) is -28 mV, which differs from the expected peak variance as around $V_{1/2}$ of Na_T. C: Mean activation channel noise for the Na_T current. Peak activation (dashed line) is 1/100 normalized conductance. At resting potential (-65 mV), the peak level of noise drops to 1/300.

4.5 Numerical Simulations: Markov-based Channel Simulations

The stochastic fluctuation in a single dynamic gating variable, from its normative value, was estimated from a Markov Chain Monte Carlo simulation (1000 trials). The variance is calculated from the trials and the variance is plotted against voltage to observe the channel model's variance. The average Na_T activation gating (Fig. 4.2A, black trace) and 100 individual gates (Fig. 4.2A, red trace) from the Markov-based ion channel simulation demonstrate the variance in channel gating. The region in the gating that shows the highest

variance (Figure 4.2B) occurs around $V_{1/2}$ (-28 mV), which is more depolarized than expected for typical Na_T channel (-45 mV). For 1000 repeated trials, average channel noise from 100 Na_T activation gates were estimated and detrended (Figure 4.2C). The peak in noise occurred at $V_{1/2}$ (-28 mV) with a normalized conductance of 1/100. Across a membrane voltage range from -40mV to 0 mV (covering 20 mV on either side of $V_{1/2}$, i.e., $V_{1/2}$ pm 20 mV), the channel noise decreases in the tails to about $3 \times 10^{-}3$. Between -70 and -60 mV, at the level of the resting membrane potential, the noise in the conductance is very small, at the order around 3.33×10^{-3} of maximum conductance.

4.6 Stochastic Implementation Motivation

Recall that the goal of the model is to reproduce stochastic behavior seen in the experimental data. In the literature, previous work in introducing stochastic behavior in biophysical models is discussed above. Findings from Schwalger and colleagues [55] have concluded that the time scale of the adaptive current is more important in determining the serial correlation coefficients at lag one than the noise terms. Their work describes two models: 1) a perfect integrate-and-fire model with an adaptive current, and a Hodgkin Huxley-type model with an adaptive current. In addition, they included additive noise terms in the equation for the change in voltage and the change in adaptive current. They have found that, in comparison to a deterministic model, positively correlated noise introduced into the system produces positively correlated inter-spike intervals and eliminates the negative correlation coefficients seen in the deterministic case. Thus, a direct effect occurs with their stochastic model, with statistics of the noise being passed directly to the ISI correlation of adjacent spikes. In other words, positively correlated noise produces positive SCCs at lag 1. However, Guler [71] had shown that introducing correlated noise into the channel conductance, rather than the channel gating equations of the Hodgkin Huxley model, more successfully matches the spiking behavior of experimental recordings than previous Langevin approaches to a biophysical

model.

A report from our lab by Sidhu et al. [10] has demonstrated that correlated noise in the dynamic threshold can lead to a change in ISI correlations and associated spiking behaviors, such as burstiness. They have derived a relationship between the correlation of noise between spikes and their SCCs. Although the dynamic threshold in the spiking model is mathematical, the underlying mechanism is thought to exist in a voltage gated ion current. If this so-called adaptation current occurs, then it seems reasonable to introduce spike correlated/anti-correlated noise into the suspected channel. In the INCF dataset, jitter in the spike timing is likely affected by the M current, but there are questions of biophysical plausibility about the implementation of noise. There is a body of literature showing that modulation of the M-current is due to receptor-mediated or calcium-dependent pathways (modal gating [114]), and occurs at longer time scales of 0.1 to 10 seconds [19], [115].

Although the mechanisms of the modulation after a spike are not known, we postulate that modulation, if it were to occur, would be constant between the spikes. Previous work (Chapter 3) demonstrates that the M currents contribute to the dynamic threshold. Our approach, as described in the next section, is to alter the maximum conductance of the neuron after a spiking event has occurred.

4.7 Model Details: Stochastic Hodgkin Huxley Model

The change in the M current's maximum conductance occurs after each spike. The underlying biophysical mechanism of the dependent change is attributed to modal gating. In modal gating, the change in channel opening rate is thought to be modulated by messengers generated by spike firing [114]. One possible scheme is related to signaling between the sodium channels and the M current, as speculated by Pan [80]. It may be biophysically possible, although never experimentally observed, for communication about a spiking occurrence from a large influx of Sodium ion channels to occur with the M-channels. This mechanism is consistent

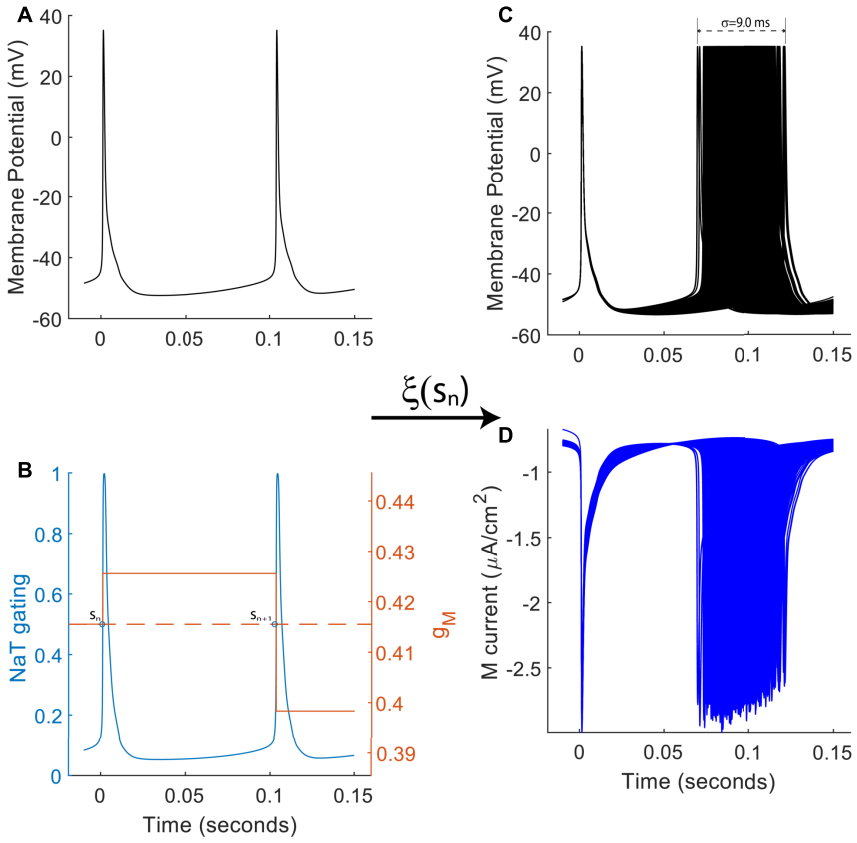

Figure 4.3: Stochastic model implementation a) Spike-triggered membrane voltage at neuron. Upon activation of fast Sodium (b) alters the opening probability of the M-channel and $\xi(s_n)$ influences activation of the M current. The resulting change in the M-channel permeability leads to noise in the interspike interval statistics. c) Implementation of the simulation neuron to a constant step-current stimulus. Overlaid spike-triggered membrane voltage produces spike jitter governed by $\xi(s_n)$

with the idea of modal gating in addition to the fact that the Nav1 and Kv7.2/7.3 channels are colocalized via the Ankyrin-G binding protein [80] and proceeds as follows:

Let $\xi(s_n)$ be a random variable, a be a constant reflecting the noise correlation between action potentials, and ϵ_n be a white noise process with zero mean and finite variance. During the rise of Na_T activation, the event $r = n_0$ occurs when activation reaches 0.5, and the following is initiated:

$$\xi(s_n) = a \cdot \xi(s_{n-1}) + \epsilon(s_n) \tag{4.1}$$

When the activation gating of Na_T is greater than 0.5 on the upslope, the following change in maximum conductance occurs (M-current):

$$\widetilde{g_m}(r) = g_m + \epsilon(s_n) \tag{4.2}$$

where g_m is the nominal value of the M-channel maximum conductance.

The process repeats for subsequent action potentials. The parameter a is a feedback parameter which carries the memory of preceding ISIs. The equation for $\xi(s_n)$ is a first-order autoregressive process, similar to the noise process used by Sidhu et al. [10] to shift the spiking threshold. My stochastic Minimum Hodgkin-Huxley (MHH) model (Equations 4.1-4.2) is a straightforward approach to the adjustment of the adaptation current. It contains two free parameters, "a", and the variance of ϵ. A diagram of the implementation is shown in Figure 4.3.

4.8 Numerical Simulation: Noise Introduced into a Biophysical Model

Introduction of noise into the M-current was achieved by perturbing the maximum conductance parameter after each spike. After the activation gate of Na_T reaches half its maximum value, the maximum conductance is changed by adding scaled noise to a range of parameters obtained from the Markov-based simulations and the process repeats for subsequent spikes. A search across different parameter values in the noise model were compared to the experimental data. The varying parameters were noise scaling and the correlation parameter. The correlation parameter 'a' ranged between -0.9 and 0.9. The parameters selected for the results are: a=0.4, $\mathrm{Var}(\epsilon) = 10^{-4}$.

The model is given an input of frozen synaptic current stimulus, from the INCF experimental data. The frozen noise stimulus was repeatedly presented to the model neuron for

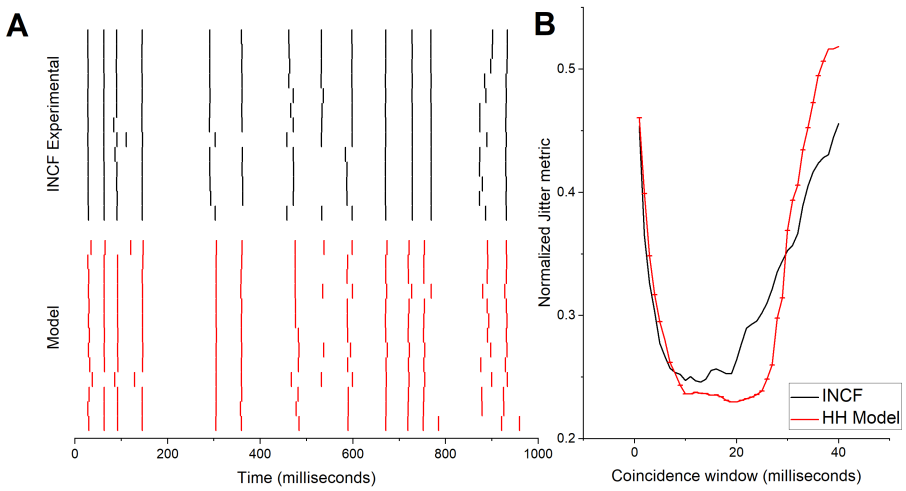

Figure 4.4: Accuracy of stochastic model to experimental data. a) raster plot of experimental data (above, black) and model (below, red) show individual spike variability. b) modified coincidence metric to evaluate jitter across 13 trials for the model (red) and experimental data (black). Repeated sets of trials (n=14) of the model were used to measure the consistency of the model jitter.

a total of 13 trials, and the output is depicted in a raster plot of the spikes (Fig. 4.4A, red). For comparison the raster plot from the experimental data is also shown (Fig. 4.4A, black). Full stimuli response for the trials is shown in Appendix (A.2) for reference. The implemented model's spiking jitter appears to fit the INCF data quite well, with qualitative features retained. For example, the 8th spike in the set of spikes in the simulation contains a failure-to-spike condition in a fraction of the trials. When considering the similarity of the model to the experimental data, the modified coincidence metric (see Methods for evaluation) calculates the normalized distance between coincident spikes across all trials. We plot the metric for different coincidence windows to see where the model fails to capture behavior seen in the experimental data.

From 1-10 ms of the coincidence window, the model (red) precisely follows the experimental jitter (black). At values exceeding this range, the model begins to deviate. Next, we asked if this model responds to injected stimuli as described by Mainen & Sejnowski (1995). Their work on the behavior of neurons under constant DC step current stimuli and frozen noise of

increasing variance revealed the following: in the absence of fluctuating input (i.e., DC step input), the timing consistency of neurons deteriorates and produces decorrelation over time as the stimuli is presented (i.e., low reliability and precision). However, when frozen noise is introduced, the reliability and precision of the spike increases for larger noise variance. This finding has described neurons spike reliably for synaptic input.

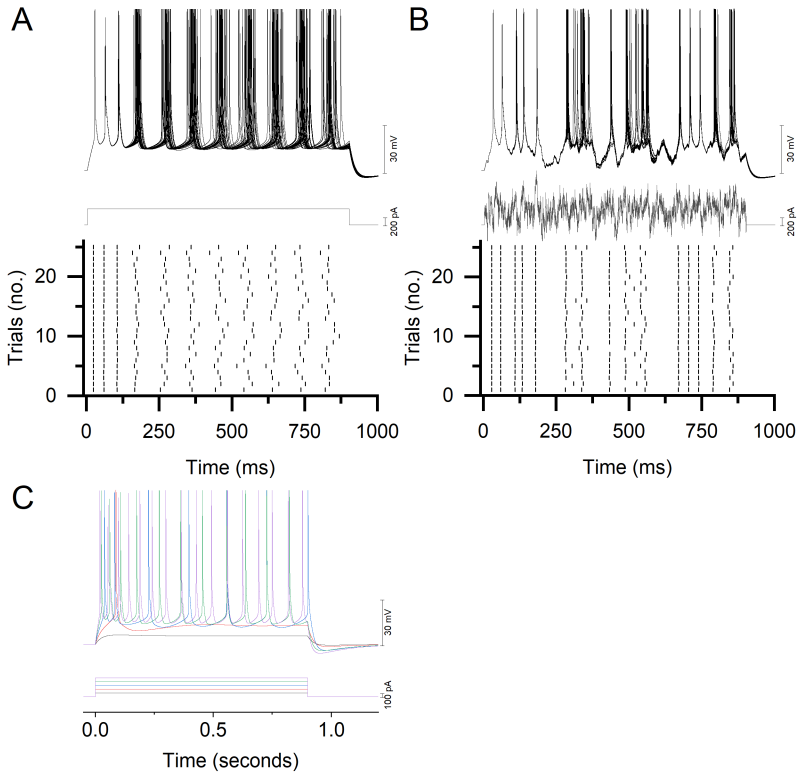

Figure 4.5: Consistency in findings of neuron firing reliability. Comparison between findings of Mainen & Sejnowski, 1995, upon repeated stimulation of a constant step current (a) and one with added noise (b). A step current alone produces spike timing that decorrelates over time. Adding noise of sufficient variability produces reliable spike firing. (c) model response against varying step current amplitudes.

In Mainen & Sejnowski's Figure 1A, they show that a DC pulse of 150 pA stimulus produces spiking at a firing rate of 14 Hz that decorrelates over time. In their Figure 1B, with a 'Gaussian white stimulus' with a $\mu = 150$ pA and $\sigma = 100$ pA, spiking is very precise over time, across multiple trials. A 900 ms current stimuli is injected into the model neuron and the membrane voltage, along with the raster for 25 trials are simulated. In our model, under

DC stimuli at 150 pA, the model does not produce the same firing rate (2 Hz, see Fig. 4.5C). However, if we increase amplitude to match firing rate (400 pA), the model reproduces spiking behavior similar to their Figure 1A (Fig. 4.5A). Due to differences in stimulation amplitude attributed to experimental preparation, noise was scaled by its coefficient of variation. For output under frozen noise, white noise was filtered with an exponential filter, in a manner identical to the described paper: $\tau = 3$ milliseconds, $\mu = 400$ pA, $\sigma = 183$ pA. For frozen noise input (Fig. 4.5B), precise spike times are observed, consistent with previous findings. To test for reliability in the metric and model, 10 sets of 13 trials of the model to the INCF data was subsequently run to observe the variation in the model, and confirms that its average jitter is not trial-dependent.

Finally, to observe the model's effect on spike-timing correlations, we compared ISI serial correlation coefficients to the theoretical as described by Sidhu et al. [10]. In their work, correlated noise ("a" parameter) is related to a neuron's serial correlation coefficient by the following equation:

$$\rho_k = \frac{a^{k-1}\ (1-a)}{2}, k \geq 1$$

where k is the kth lag from any given ISI and is denoted here as the theoretical value of ρ. This equation can be plotted across values of "a" between -1 and 1 for any k. In practice, estimating the value of 'a' in experimental data requires a large amount of spike times under constant current steps. In the model simulation, calculation of ISI correlations requires many spikes, and a step current stimulus of sufficient amplitude to produce a firing rate of around 10 Hz was simulated for 200 seconds. The calculated correlation coefficient of the first lag (ρ_1) plotted against "a" and compared to the theoretical value obtained from the equation above (Fig. 4.6).

Altering the maximum conductance in M-current produces negative ISI correlations compared to theoretical values. For the plot, the noise correlation (a) along abscissa ranged from -0.9 to 0.9 and ρ_1 is the correlation between a given ISI and the following ISI. The theoretical value of ρ_1 (Figure 4.6, black line) is obtained from the equation provided by

Sidhu et al. [10]. Noise in the maximum conductance of the M-current with a noise scaling value of 0.01 shows that I can reproduce the first ISI correlation accurately for a range of "a" values, even for a small perturbation in the model parameters. Note that the sign of the correlation variable "a" determines the value of ρ_1 (Fig. 4.5). When $a < 0$, $\rho_1 < -0.5$, and when $a > 0$, $\rho_1 > -0.5$. This was reported by Sidhu et al. [10]. However, when evaluating the difference in ISIs, the jitter for the model (13 ms) differs from the experimental data (11.97 ms, not shown).

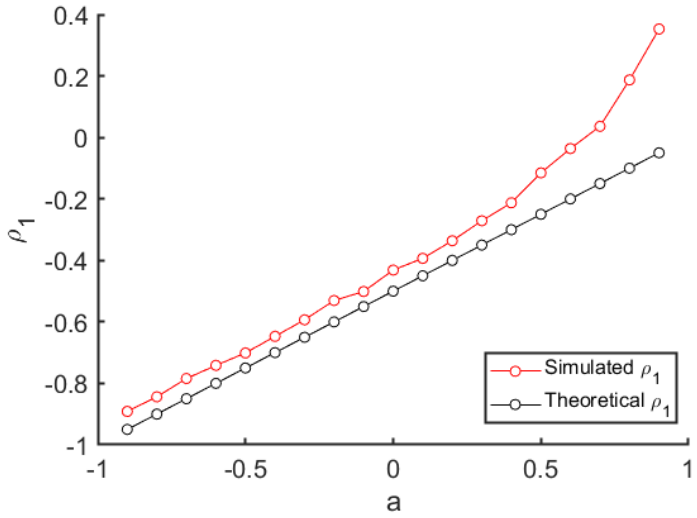

Figure 4.6: The stochastic model describes a stochastic threshold model proposed by Sidhu et al. a) a constant step current was used as the input stimulus to the model and run for 200 seconds to obtain around 3500 spikes. The serial correlation coefficients were calculated from the spike times, the first SCC (ρ_1) was plotted for varying "a" and overlaid with the expected value, "a" estimated by Sidhu et al. [10]

4.9 Discussion

The model used in this chapter is an extension of the deterministic model described in chapter 2. The approach in development of the model aims to represent jitter in real neurons, constrained to biophysical processes that are known to occur. The effect of the M-current in membrane excitability is well known. Further, the M-current is modulated by many different pathways [19] and is implicated in metabolic regulation of spiking [11], [116]. The choice of modifying the maximum conductance of the M-current, based on the activity of Na_T is consistent with the ideas proposed in modal gating of the M-current. The mechanisms of modal gating and how it modulates the M-current are not fully known. What is known is that the M-current is modulated through receptor binding and by intracellular calcium. This is of particular interest since the KCNQ channel is linked to the sodium currents through the anchoring protein. This link, we speculate, can introduce a correlated noise after a spike occurs. With the M-channel partially conducting or fully opening there is a possible way that it can alter its opening and closing rate. The M-current can switch between two or three modes, at rates lower than those found in the traditional open and close scheme of the channel. This rate can be influenced experimentally by introducing acetylcholine into the cell [114], [117]. How this affects excitability is partially known from the work of Brown [13] where excitability of a cell increases for increasing concentration via M-current suppression. Some mechanisms of interest are the PIP2 pathway and intracellular calcium concentration. In contrast to other ion channels, PIP2 binding leads to an increased activation of the channel. Nevertheless, the exact mechanisms related to modal gating in relation to spiking are not known.

The model proposed in this thesis is conjectural, with mechanisms involved in the regulation of the M-current being responsible for its altered conductance. The results of the Markov-channel simulation were used to observe the amount of variance across different voltages by channel noise to estimate the amount of change into, ultimately, the conductance.

The raster shown above Fig 4.5A shows that the model can match the jitter to the

experimental data. For the 21.49 seconds of noise, a more viable metric is desired. A coincidence metric is a value from 0 to 1, scaled based on the coincidence window length to allow a comparison for the complete set of data. The model's average jitter metric is almost identical to the experimental data for jitter less than 10 ms and begins to deviate for larger windows. This indicates that a small change in conductance of the M-current (additive noise scaled 1/100 of maximum conductance) is plausibly the source of jitter for small time scales. At larger coincidence windows, there exists spiking jitter in the data that is not factored in the model.

As previously described, Mainen and Sejnowski [60] had shown that repeated stimulation by a step current stimulus produces spike jitter precision that decorrelates over time. However, when a frozen stimulus is used that resembles synaptic activity, repeated trials on the neuron produce precise spike timing. To confirm the model's behavior to such types of stimuli, it is expected that the stochastic model will produce plots identical to that shown by Mainen and Sejnowski. Metrics discussed in their report, such as precision and reliability, were excluded due to its large variability from neuron to neuron and would not provide anything meaningful. In comparing the behavior of the model to noise, differences in stimulus current amplitude were observed. This difference could be partially explained by the methods of the experimental recordings. In the data the model was fitted for, the "liquid junction potential between the ACSF and the intracellular solution (ICS) was around 12 mV and not corrected for [2]," indicating that a shunt in the current could have occurred, leading to less current injected into the neuron. We had applied an ad-hoc correction by matching neural firing rate and coefficient of variation of stimulus noise. With the correction, the model can reproduce the findings of Mainen and Sejnowski with our stochastic model.

Finally, a stochastic adaptive current in a Minimum Hodgkin Huxley (MHH) type model can produce negative correlation behavior as seen in Sidhu et al. [10]. We speculate that a stochastic adaptive current can produce the behavior seen in a stochastic dynamic threshold model. The complication is that the Hodgkin Huxley-type model equations are coupled to

the membrane voltage, and we cannot definitively say that the noise in the M-current is leading to the negative ISI correlations. Schwalger and colleagues have described that colored noise will raise the ISI correlation, but this model shows that some positively correlated noise can still produce negative serial correlation coefficients and is closer to the observations from [10]. The model's serial correlation coefficients for lag 1, however, appear to deviate for noise correlation 'a' exceeding about 0.6. It is noted that in the dataset of electric fish, noise correlation values estimated from the data do not exceed 0.6. and ongoing work agrees with this speculation (data not shown).

Chapter 5

Summary and Conclusions

The results presented in this thesis have shown that a Hodgkin Huxley-type model containing 4 defined voltage-gated ion channels (Na_T, Na_P, K_{DR}, and K_M), are the minimum number of channels needed to reproduce spike timing in neurons. A necessary channel in the model, an outward potassium current or an M-current, describes the dynamic threshold in neurons. This finding assisted the development of a stochastic extension in the next part of this thesis, where noise in the dynamic threshold is known to reproduce firing behavior in electric fish p-type afferents [10]. Findings from this research are consistent with the theory of a stochastic threshold model. The stochastic element used in this thesis is not described by the Hodgkin-Huxley equations nor channel noise alone, but from the modulation of a channel from an indetermined mechanism. The model described in this paper was aimed at action potential generation in the Axonal Initial Segment, with the goal of fitting spike times on the basis of the underlying short-term adaptation. Long-term adaptation and its mechanisms are not considered in this model. In addition, the M-current in spike timing and jitter channels have a prominent role on membrane excitability and synaptic plasticity. From the results of this study, an M-current as a channel largely responsible for spike timing and jitter, align well to the theory of optimal coding.

The model and fitting procedure used in this paper (see [16], [91], [118]) originally included

calcium channels and various potassium channels. In our work with the model in the rat cortical neurons, the model would converge to a parameter set which had large errors between the membrane potential of the recordings and the model. This effect could possibly be due to the nonlinearity of the Hodgkin Huxley-type model. Therefore, the choice to reduce the number of channels in the model to limit the number of free parameters in the model was made. That is, we reduce the model to those only contained in the axon initial segment.

The fitting procedure was challenging, and had required over 90 GB of RAM to fit 1-2 seconds of data over a period of days to complete. Even then, multiple runs had a chance to converge to a local minimum. The topic of overfitting is a problem in generalizing model results. The parameters obtained from this model were tuned specifically for the INCF dataset. The model organism is the p14 rat in layer 5. It is not known if the recordings are from thick-tufted or thin-tufted neurons. Thick-tufted neurons in juvenile rats share the same firing behavior as their mature counterpart. They are regular-firing and have less spontaneous activity. The preparation of the in vitro recordings does not appear to have prevented multi-synaptic activity, thereby leaving the possibility of network effects. On the other hand, the INCF dataset was part of a competition with the results of known models and had made comparison of model performance possible. At the time of the fittings, a dataset containing individual recordings from all cortical layers was made publicly available [36]. This preparation had used a high magnesium, low calcium concentration of ACSF, and partially blocks possible network effects [27], [119]. Attempts at generalization of the model could make use of a comprehensive dataset. The caveat to this notion is that each neuron will need to be re-tuned, either by the optimization procedure highlighted by the Abarbanel group or by hand. Models for spike timing would need to be fit in a neuron-to-neuron basis [83]. There is no parameter set that accurately predicts spike timing for all neurons, even of the same type.

Limitations from these findings may be attributed to the Hodgkin-Huxley model itself. While it is viewed as a biophysical model, is becoming less so with the more information

discovered about voltage-gated ion channels. The biophysical accuracy of the gating interactions of the Hodgkin-Huxley variables, such as the ball-and-chain model of sodium channels, has been questioned [43], [120]. In the ball-and-chain model, initial depolarization influences inactivation of the sodium channel, and there is a coupling with sodium activation that is not factored into the model.

Nevertheless, we find that the behavior of serial correlation coefficients can be introduced into a biophysical model with a stochastic M-current, where the noise communicated from the Sodium channels influences the adaptive current at subthreshold level. Questions this thesis has left unanswered include whether the stochastic implementation is directly changing the threshold and if this hypothesis extends to neurons beyond a single dataset in layer 5 cortical neurons. Most importantly, what is the key specific biophysical mechanism responsible for such change? In the following section, we suggest some future experiments that might address these questions.

5.1 Experimental Directions

In consideration to experimental techniques to find support of my model, a search of hypotheses in the literature of colored noise in membranes raised possibilities of membrane physiology experiments that may be performed. There exist a body of research that shows evidence of cooperation of ion channel clusters, within a given area of the cell, to produced colored noise in the membranes. The resulting effect on the membrane potential produces a memory component in the cell [121], [122]. However, the hypothesis in the stochastic implementation in Chapter 4 does not look at the history of the membrane voltage, but the history of spikes. It is based on a possible interaction between Na_T and M-channels. If one were to test this hypothesis, then a reasonable start would be to compare the conductance of these ion channels when the interaction would be present and absent. If correlated noise is the consequence of such an interaction, a voltage clamp experiment that observes the kinetics of Na_T and K_M

in a neuron, through pharmacological blockade of other channels, may confirm if correlated noise (i.e. the "a" parameter in the model) is caused by the interaction or by the membrane voltage, as suggested by ion cooperation. Alternatively, the introduction of proteases that degrade the cytoskeleton, particularly the Ankyrin-G binding protein, can be used to weaken the link between Na_T and K_M, and observed in voltage clamp experiments. Dynamic clamp experiments may also be key in distinguishing the source of the correlated noise.

The question of suitable preparation arises. In order to retain the relative distribution of ion channels, as observed in the AIS, I speculate that an *in-vitro* whole cell patch clamp of the AIS region can demonstrate desired results. However, targeting a specific region in the axon without labeling and imaging the AIS would be a challenge. Another possibility is to perform a preparation from an artificial expression of the AIS ion channels and scaffolding proteins in the *Xenopous* oocyte. The specifics of such a preparation are a challenge of itself, as the density of M-type channels are 10 channels per μm^2 and Sodium channels are 110-300 per μm^2 [22], but may prove an interesting endeavor into uncovering the behavior of ion channel interactions only speculated in this thesis.

5.2 Computational Directions

On the computational side, the mechanism in consideration for stochastic spike firing is the possible communication between Sodium and M-type channels, resulting in the modulation of the M-current. I have intentionally simplified the stochastic behavior due to many unknowns about modulation *in-vivo*. The M-current is believed to be regulated by many different pathways [114], which are not expressed in the Hodgkin-Huxley equations. A review of biophysical models (see [43]) addresses morphological neuron models and details the insufficiencies of them and discuss many factors, such as heterogeneity of ion channel kinetics within a neuron, use of the Hodgkin-Huxley equations and ignoring biochemical network properties. Their consideration to future experimentalists lays out a comprehensive approach

of capturing spiking behavior and individual ion kinetics. While the model in this thesis does not look at morphological or multi-compartment models, I'm inclined to believe Almog and Korngreen's proposal to explore the realm of molecular dynamics to understand neural coding [43].

Possible future directions in this work can turn toward the behavior of ion channels at a microscopic level, perhaps through Markov chain models employing modal gating [117], where interactions beyond those described in the Hodgkin-Huxley model can be investigated.

Appendix A

Supplementary Figures

Parameter	Value	Parameter	Value	Parameter	Value	Parameter	Value
Cm	1.02	gNaP	0.27	KDRina_V1	-42.93	gL	0.04
Iscale	360.46	NaP_V1	-35.77	KDRina_V2	-14.58	EL	-65.00
gNaT	38.52	NatP_V2	5.00	KDRina_V3	-6.35		
NaTm_V1	-28.87	NaP_V3	5.00	KDRina_t0	1.15		
NatTm_V2	16.28	NaP_t0	1.38	KDRina_t0	19.69		
NaTm_V3	0.50	NAP_eps	7.00	KDRina_deltasq	0.00		
NaTm_t0	0.13	ENa	50.00	gKM	0.42		
NATm_eps	0.01	gKDR	7.03	KM_V1	-20.00		
NaTm_V1	-43.87	KDRact_V1	-43.46	KM_V2	17.11		
NaTm_V2	-1.92	KDRact_V2	13.48	KM_V3	46.05		
NaTm_V3	5.00	KDRact_V3	5.00	KM_t0	55.00		
NaTh_t0	0.29	KDRact_to	0.61	KM_eps	150.00		
NaTh_eps	30.00	KDRact_eps	1.00	EK	-85.00		

Figure A.1: Minimum Hodgkin-Huxley Model Parameters for NaT (transient sodium), NaP (persistent sodium), KDR (potassium delayed rectifier), and KM (M-current). Equations follow the style of the model described in Nogaret et al [14]. It is important to note that the parameters are not correct for junction potential between the ACSF and intracellular solution. In the figure, the suffix "act" is associated with a channel's subunit activation, and "ina" is its inactivation.

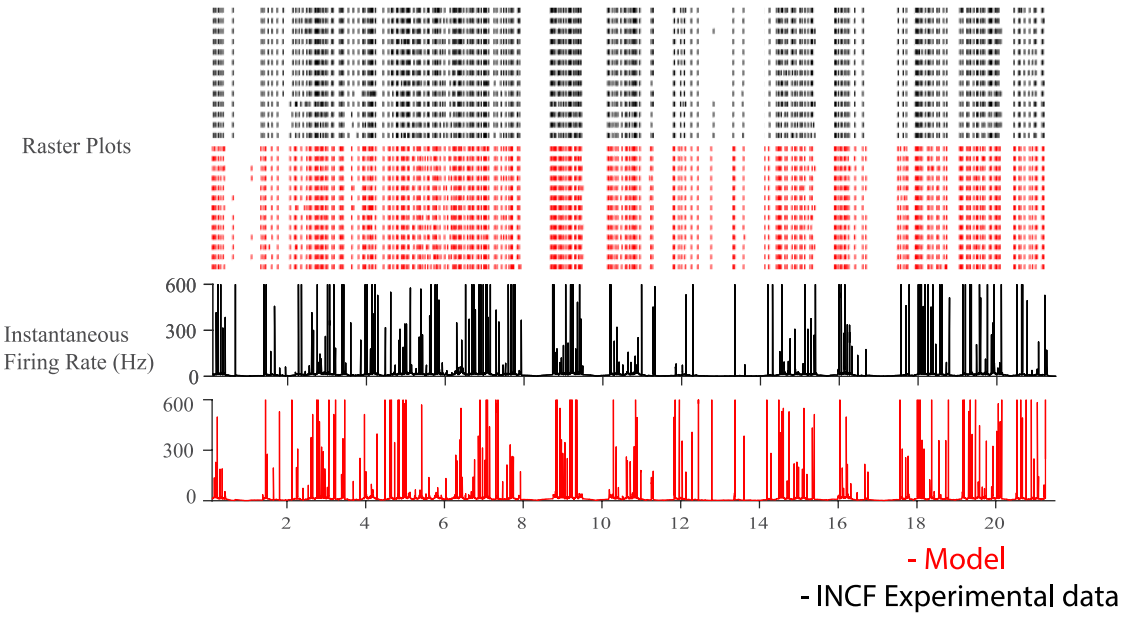

Figure A.2: Complete data of Stochastic MHH model simulations (red) compared to INCF dataset (black). Raster plots appear to show similar jitter to the model, but it is difficult to evaluate the model's ability to replicate jitter seen in the experimental data. Instantaneous firing rates, calculated from the PSTH described by [60], again show some similarities between the two. However, not much can be known from a comparison of either result.

References

[1] R. Kobayashi, "Made-to-order spiking neuron model equipped with a multi-timescale adaptive threshold," *Frontiers in Computational Neuroscience*, vol. 3, no. July, pp. 1–11, 2009.

[2] R. Naud, T. K. Berger, and B. Bathellier, "Quantitative Single-Neuron Modeling : Competition 2009," pp. 1–8, 2009.

[3] D. Attwell and S. B. Laughlin, "An energy budget for signaling in the grey matter of the brain," *Journal of Cerebral Blood Flow and Metabolism*, vol. 21, no. 10, pp. 1133–1145, 2001.

[4] T. Berger and W. B. Levy, "A mathematical theory of energy efficient neural computation and communication," *IEEE Transactions on Information Theory*, vol. 56, no. 2, pp. 852–874, 2010.

[5] E. de Boer, "On the Principle of Specific Coding," *Journal of Dynamic Systems, Measurement, and Control*, vol. 95, no. 3, pp. 265–273, 1973, ISSN: 00220434.

[6] N. Brunel and M. C. W. van Rossum, "Lapicque's 1907 paper: from frogs to integrate-and-fire," *Biological Cybernetics*, vol. 97, no. 5-6, pp. 337–339, 2007.

[7] C. C. Gielen, G. H. Hesselmans, and P. I. Johannesma, "Sensory interpretation of neural activity patterns," *Mathematical Biosciences*, vol. 88, no. 1, pp. 15–35, 1988.

[8] W. Bialek, F. Rieke, R. R. De Ruyter Van Steveninck, and D. Warland, "Reading a neural code," *Science*, vol. 252, no. 5014, pp. 1854–1857, 1991.

[9] F. Gabbiani and S. Cox, in. 2010, ch. Reverse-Correlation and Spike Train Decoding, pp. 335–341, ISBN: 978-0-12-374882-9.

[10] R. S. Sidhu, E. C. Johnson, D. L. Jones, and R. Ratnam, "A dynamic spike threshold with correlated noise predicts observed patterns of negative interval correlations in neuronal spike trains," *Biological Cybernetics*, vol. 116, no. 5, pp. 611–633, 2022.

[11] D. L. Jones, E. C. Johnson, and R. Ratnam, "A stimulus-dependent spike threshold is an optimal neural coder," *Frontiers in Computational Neuroscience*, vol. 9, no. June, 2015.

[12] R. Ranjan, E. Logette, M. Marani, M. Herzog, V. Tâche, E. Scantamburlo, V. Buchillier, and H. Markram, "A Kinetic Map of the Homomeric Voltage-Gated Potassium Channel (Kv) Family," *Frontiers in Cellular Neuroscience*, vol. 13, no. August, pp. 1–25, 2019.

[13] D. A. Brown and P. R. Adams, "Muscarinic suppression of a novel voltage-sensitive K+ current in a vertebrate neurone.," *Nature*, vol. 283, no. 5748, pp. 673–6, 1980.

[14] A. Nogaret, C. D. Meliza, D. Margoliash, and H. D. I. Abarbanel, "Automatic Construction of Predictive Neuron Models through Large Scale Assimilation of Electrophysiological Data," *Scientific Reports*, vol. 6, no. 1, p. 32 749, 2016.

[15] S. Ramaswamy and H. Markram, "Anatomy and physiology of the thick-tufted layer 5 pyramidal neuron," *Frontiers in Cellular Neuroscience*, vol. 9, no. June, pp. 1–29, 2015.

[16] C. D. Meliza, M. Kostuk, H. Huang, A. Nogaret, D. Margoliash, and H. D. I. Abarbanel, "Estimating parameters and predicting membrane voltages with conductance-based neuron models," *Biological Cybernetics*, vol. 108, no. 4, pp. 495–516, 2014.

[17] E. Hay, S. Hill, F. Schürmann, H. Markram, and I. Segev, "Models of neocortical layer 5b pyramidal cells capturing a wide range of dendritic and perisomatic active properties," *PLoS Computational Biology*, vol. 7, no. 7, 2011.

[18] N. Eijkelkamp, J. E. Linley, M. D. Baker, M. S. Minett, R. Cregg, R. Werdehausen, F. Rugiero, and J. N. Wood, "Neurological perspectives on voltage-gated sodium channels," *Brain*, vol. 135, no. 9, pp. 2585–2612, 2012.

[19] F. Barros, P. Domínguez, and P. de la Peña, "Cytoplasmic domains and voltage-dependent potassium channel gating," *Frontiers in Pharmacology*, vol. 3 MAR, no. March, pp. 1–15, 2012.

[20] T. Kiss, "Persistent Na-channels: Origin and function: A review János Salánki memory lecture," *Acta Biologica Hungarica*, vol. 59, no. SUPPL. Pp. 1–12, 2008.

[21] A. Battefeld, B. T. Tran, J. Gavrilis, E. C. Cooper, and M. H. Kole, "Heteromeric Kv7.2/7.3 channels differentially regulate action potential initiation and conduction in neocortical myelinated axons," *Journal of Neuroscience*, vol. 34, no. 10, pp. 3719–3732, 2014.

[22] M. H. P. Kole and G. J. Stuart, "Signal Processing in the Axon Initial Segment," *Neuron*, vol. 73, no. 2, pp. 235–247, 2012.

[23] M. H. P. Kole, S. U. Ilschner, B. M. Kampa, S. R. Williams, P. C. Ruben, and G. J. Stuart, "Action potential generation requires a high sodium channel density in the axon initial segment," *Nature Neuroscience*, vol. 11, no. 2, pp. 178–186, 2008.

[24] A. S. Shai, C. A. Anastassiou, M. E. Larkum, and C. Koch, "Physiology of Layer 5 Pyramidal Neurons in Mouse Primary Visual Cortex: Coincidence Detection through Bursting," *PLoS Computational Biology*, vol. 11, no. 3, pp. 1–18, 2015.

[25] C. Rock and A. j. Apicella, "Callosal Projections Drive Neuronal-Specific Responses in the Mouse Auditory Cortex," *Journal of Neuroscience*, vol. 35, no. 17, pp. 6703–6713, 2015.

[26] B. J. Slater, S. K. Sons, G. Yudintsev, C. M. Lee, and D. A. Llano, "Thalamocortical and intracortical inputs differentiate layer-specific mouse auditory corticocollicular neurons," *Journal of Neuroscience*, vol. 39, no. 2, pp. 256–270, 2019.

[27] D. A. Llano and S. M. Sherman, "Differences in intrinsic properties and local network connectivity of identified layer 5 and layer 6 adult mouse auditory corticothalamic neurons support a dual corticothalamic projection hypothesis," *Cerebral Cortex*, vol. 19, no. 12, pp. 2810–2826, 2009.

[28] K. D. Games and J. A. Winer, "Layer V in rat auditory cortex: Projections to the inferior colliculus and contralateral cortex," *Hearing Research*, vol. 34, no. 1, pp. 1–25, 1988.

[29] A. L. Hodgkin and A. F. Huxley, "A quantitative description of membrane current and its application to conduction and excitation in nerve," *Journal of Physiology*, vol. 117, no. 4, pp. 500–544, 1952.

[30] W. Gerstner, W. M. Kistler, R. Naud, and L. Paninski, *Neuronal Dynamics*. Cambridge University Press, 2014, ISBN: 9781107060838.

[31] L. Badel, S. Lefort, T. K. Berger, C. C. Petersen, W. Gerstner, and M. J. Richardson, "Extracting non-linear integrate-and-fire models from experimental data using dynamic I-V curves," *Biological Cybernetics*, vol. 99, no. 4-5, pp. 361–370, 2008.

[32] L. Badel, S. Lefort, R. Brette, C. C. H. Petersen, W. Gerstner, and M. J. E. Richardson, "Dynamic I-V curves are reliable predictors of naturalistic pyramidal-neuron voltage traces.," *Journal of neurophysiology*, vol. 99, no. 2, pp. 656–66, 2008.

[33] J. W. Pillow, J. Shlens, L. Paninski, A. Sher, A. M. Litke, E. J. Chichilnisky, and E. P. Simoncelli, "Spatio-temporal correlations and visual signalling in a complete neuronal population," *Nature*, vol. 454, no. 7207, pp. 995–999, 2008.

[34] E. Izhikevich, "Simple model of spiking neurons," *IEEE Transactions on Neural Networks*, vol. 14, no. 6, pp. 1569–1572, 2003.

[35] J. Benda, L. Maler, and A. Longtin, "Linear versus nonlinear signal transmission in neuron models with adaptation currents or dynamic thresholds," *Journal of Neurophysiology*, vol. 104, no. 5, pp. 2806–2820, 2010.

[36] P. M. Harrison, L. Badel, M. J. Wall, and M. J. Richardson, "Experimentally Verified Parameter Sets for Modelling Heterogeneous Neocortical Pyramidal-Cell Populations," *PLoS Computational Biology*, vol. 11, no. 8, pp. 1–23, 2015.

[37] M. J. Chacron, "Nonlinear Information Processing in a Model Sensory System," *Journal of Neurophysiology*, vol. 95, no. 5, pp. 2933–2946, 2006.

[38] Z. F. Mainen and T. J. Sejnowski, "Influence of dendritic structure on firing pattern in model neocortical neurons," *Nature*, vol. 382, no. 6589, pp. 363–366, 1996.

[39] E. Iavarone, J. Yi, Y. Shi, B. J. Zandt, C. O'reilly, W. Van Geit, C. Rössert, H. Markram, and S. L. Hill, "Experimentally-constrained biophysical models of tonic and burst firing modes in thalamocortical neurons," *PLoS Computational Biology*, vol. 15, no. 5, pp. 1–23, 2019.

[40] S. Druckmann, Y. Banitt, A. Gidon, and F. Schürmann, "A novel multiple objective optimization framework for constraining conductance-based neuron models ...," *Frontiers in neuroscience*, vol. 1, no. 1, 2007.

[41] A. T. Schaefer, M. E. Larkum, B. Sakmann, and A. Roth, "Coincidence detection in pyramidal neurons is tuned by their dendritic branching pattern.," *Journal of Neurophysiology*, vol. 89, no. 6, pp. 3143–3154, 2003.

[42] M. Almog and A. Korngreen, "A quantitative description of dendritic conductances and its application to dendritic excitation in layer 5 pyramidal neurons.," *Journal of Neuroscience*, vol. 34, no. 1, pp. 182–96, 2014.

[43] M. Almog and A. Korngreen, "Is realistic neuronal modeling realistic?" *Journal of Neurophysiology*, vol. 116, no. 5, pp. 2180–2209, 2016.

[44] M. J. Chacron, A. Longtin, and L. Maler, "Negative Interspike Interval Correlations Increase the Neuronal Capacity for Encoding Time-Dependent Stimuli," *Journal of Neuroscience*, vol. 21, no. 14, pp. 5328–5343, 2001.

[45] B. Wark, B. N. Lundstrom, and A. Fairhall, "Sensory adaptation," *Current Opinion in Neurobiology*, vol. 17, no. 4, pp. 423–429, 2007. arXiv: `NIHMS150003`.

[46] A. L. Fairhall, G. D. Lewen, W. Bialek, and R. R. de Ruyter van Steveninck, "Efficiency and ambiguity in an adaptive neural code," *Nature*, vol. 412, no. 6849, pp. 787–792, 2001.

[47] H. D. Landahl, "Theory of the distribution of response times in nerve fibers," *The Bulletin of Mathematical Biophysics*, vol. 3, no. 4, pp. 141–147, 1941.

[48] C. Geisler and J. M. Goldberg, "A Stochastic Model of the Repetitive Activity of Neurons," *Biophysical Journal*, vol. 6, no. 1, pp. 53–69, 1966.

[49] M. E. Nelson, Z. Xu, and J. R. Payne, "Characterization and modeling of P-type electrosensory afferent responses to amplitude modulations in a wave-type electric fish," *Journal of Comparative Physiology - A Sensory, Neural, and Behavioral Physiology*, vol. 181, no. 5, pp. 532–544, 1997.

[50] R. Ratnam and M. E. Nelson, "Nonrenewal Statistics of Electrosensory Afferent Spike Trains : Implications for the Detection of Weak Sensory Signals," *J Neurosci*, vol. 20, no. 17, pp. 6672–6683, 2000.

[51] M. J. Chacron, K. Pakdaman, and A. Longtin, "Interspike interval correlations, memory, adaptation, and refractoriness in a leaky integrate-and-fire model with threshold fatigue," *Neural Computation*, vol. 15, no. 2, pp. 253–278, 2003.

[52] M. J. Chacron, B. Lindner, and A. Longtin, "Noise Shaping by Interval Correlations Increases Information Transfer," *Physical Review Letters*, vol. 92, no. 8, pp. 1–4, 2004.

[53] M. J. Chacron, "Feedback and Feedforward Control of Frequency Tuning to Naturalistic Stimuli," *Journal of Neuroscience*, vol. 25, no. 23, pp. 5521–5532, 2005.

[54] M. J. Chacron, L. Maler, and J. Bastian, "Electroreceptor neuron dynamics shape information transmission," *Nature Neuroscience*, vol. 8, no. 5, pp. 673–678, 2005.

[55] T. Schwalger, K. Fisch, J. Benda, and B. Lindner, "How noisy adaptation of neurons shapes interspike interval histograms and correlations," *PLoS Computational Biology*, vol. 6, no. 12, 2010.

[56] J. Platkiewicz and R. Brette, "Impact of Fast Sodium Channel Inactivation on Spike Threshold Dynamics and Synaptic Integration," *PLoS Computational Biology*, vol. 7, no. 5, 2011.

[57] S. A. Prescott and T. J. Sejnowski, "Spike-Rate Coding and Spike-Time Coding Are Affected Oppositely by Different Adaptation Mechanisms," *Journal of Neuroscience*, vol. 28, no. 50, pp. 13 649–13 661, 2008.

[58] J. Benda and A. V. M. Herz, "A Universal Model for Spike-Frequency Adaptation," *Neural Computation*, vol. 15, no. 11, pp. 2523–2564, 2003.

[59] Y. H. Liu and X. J. Wang, "Spike-frequency adaptation of a generalized leaky integrate-and-fire model neuron," *Journal of Computational Neuroscience*, vol. 10, no. 1, pp. 25–45, 2001.

[60] Z. F. Mainen and T. J. Seinowski, "Reliability of spike timing in neocortical neurons," *Science*, vol. 268, no. 5216, pp. 1503–1506, 1995.

[61] R. H. Cudmore, L. Fronzaroli-Molinieres, P. Giraud, and D. Debanne, "Spike-Time Precision and Network Synchrony Are Controlled by the Homeostatic Regulation of the D-Type Potassium Current," *Journal of Neuroscience*, vol. 30, no. 38, pp. 12 885–12 895, 2010.

[62] H. R. Leuchtag, Ed., *Voltage-Sensitive Ion Channels*. Dordrecht: Springer Netherlands, 2008, ISBN: 978-1-4020-5524-9.

[63] L. J. DeFelice and A. Isaac, "Chaotic states in a random world: Relationship between the nonlinear differential equations of excitability and the stochastic properties of ion channels," *Journal of Statistical Physics*, vol. 70, no. 1-2, pp. 339–354, 1993.

[64] J. Clay and L. DeFelice, "Relationship between membrane excitability and single channel open-close kinetics," *Biophysical Journal*, vol. 42, no. 2, pp. 151–157, 1983.

[65] E. Skaugen and L. Walløe, "Firing behaviour in a stochastic nerve membrane model based upon the Hodgkin-Huxley equations.," *Acta physiologica Scandinavica*, vol. 107, no. 4, pp. 343–63, 1979.

[66] J. H. Goldwyn, N. S. Imennov, M. Famulare, and E. Shea-Brown, "Stochastic differential equation models for ion channel noise in Hodgkin-Huxley neurons," *Physical Review E - Statistical, Nonlinear, and Soft Matter Physics*, vol. 83, no. 4, pp. 1–16, 2011. arXiv: 1009.4172.

[67] B. Sengupta, S. B. Laughlin, and J. E. Niven, "Comparison of Langevin and Markov channel noise models for neuronal signal generation," *Physical Review E - Statistical, Nonlinear, and Soft Matter Physics*, vol. 81, no. 1, pp. 1–12, 2010. arXiv: 0912.3221.

[68] J. A. White, J. T. Rubinstein, and H. Mino, "Response: Implementation issues in approximate methods for stochastic hodgkin-huxley models," *Annals of Biomedical Engineering*, vol. 35, no. 2, p. 319, 2007.

[69] I. C. Bruce, "Implementation issues in approximate methods for stochastic hodgkin-huxley models," *Annals of Biomedical Engineering*, vol. 35, no. 2, pp. 315–318, 2007.

[70] S. Pu and P. J. Thomas, "Fast and accurate langevin simulations of stochastic hodgkin-huxley dynamics," *Neural Computation*, vol. 32, no. 10, pp. 1775–1835, 2020. arXiv: 2005.10598.

[71] M. Güler, "Stochastic Hodgkin-Huxley equations with colored noise terms in the conductances.," *Neural computation*, vol. 25, no. 1, pp. 46–74, 2013.

[72] M. D. McDonnell and D. Abbott, "What is stochastic resonance? Definitions, misconceptions, debates, and its relevance to biology," *PLoS Computational Biology*, vol. 5, no. 5, 2009.

[73] G. Schmid, I. Goychuk, and P. Hänggi, "Stochastic resonance as a collective property of ion channel assemblies," *Europhysics Letters*, vol. 56, no. 1, pp. 22–28, 2001. arXiv: 0106036 [physics].

[74] A. Longtin, "Stochastic resonance in neuron models," *Journal of Statistical Physics*, vol. 70, no. 1-2, pp. 309–327, 1993.

[75] N. S. Jayant, "Digital coding of speech waveforms: Pcm, dpcm, and dm quantizers," 1974.

[76] B. C. Suh and B. Hille, "PIP2 is a necessary cofactor for ion channel function: How and why?" *Annual Review of Biophysics*, vol. 37, pp. 175–195, 2008.

[77] E. J. Dickson, B. H. Falkenburger, and B. Hille, "Quantitative properties and receptor reserve of the IP3 and calcium branch of Gq-coupled receptor signaling," *Journal of General Physiology*, vol. 141, no. 5, pp. 521–535, 2013.

[78] B. H. Falkenburger, E. J. Dickson, and B. Hille, "Quantitative properties and receptor reserve of the DAG and PKC branch of Gq-coupled receptor signaling," *Journal of General Physiology*, vol. 141, no. 5, pp. 537–555, 2013.

[79] C. Leterrier, "The Axon Initial Segment: An Updated Viewpoint.," *The Journal of Neuroscience*, vol. 38, no. 9, pp. 2135–2145, Feb. 2018.

[80] Z. Pan, T. Kao, Z. Horvath, J. Lemos, J. Y. Sul, S. D. Cranstoun, V. Bennett, S. S. Scherer, and E. C. Cooper, "A common ankyrin-G-based mechanism retains KCNQ and Na V channels at electrically active domains of the axon," *Journal of Neuroscience*, vol. 26, no. 10, pp. 2599–2613, 2006.

[81] P. M. Jenkins, N. Kim, S. L. Jones, W. C. Tseng, T. M. Svitkina, H. H. Yin, and V. Bennett, "Giant ankyrin-G: A critical innovation in vertebrate evolution of fast and integrated neuronal signaling," *Proceedings of the National Academy of Sciences of the United States of America*, vol. 112, no. 4, pp. 957–964, 2015.

[82] L. M. Palmer and G. J. Stuart, "Site of action potential initiation in layer 5 pyramidal neurons," *Journal of Neuroscience*, vol. 26, no. 6, pp. 1854–1863, 2006.

[83] R. Naud and W. Gerstner, "Can we predict every spike?" *INCF*, vol. 26, no. 4, p. 681, 2011.

[84] T. Olsen, A. Capurro, N. Pilati, C. H. Large, and M. Hamann, "Kv3 K+ currents contribute to spike-timing in dorsal cochlear nucleus principal cells," *Neuropharmacology*, vol. 133, pp. 319–333, May 2018.

[85] E. C. Johnson, D. L. Jones, and R. Ratnam, "A minimum-error, energy-constrained neural code is an instantaneous-rate code," *Journal of Computational Neuroscience*, vol. 40, no. 2, pp. 193–206, 2016.

[86] R. Azouz and C. M. Gray, "Dynamic spike threshold reveals a mechanism for synaptic coincidence detection in cortical neurons in vivo," *Proceedings of the National Academy of Sciences of the United States of America*, vol. 97, no. 14, pp. 8110–8115, 2000.

[87] R. Kobayashi and K. Kitano, "Impact of slow K+ currents on spike generation can be described by an adaptive threshold model," *Journal of Computational Neuroscience*, vol. 40, no. 3, pp. 347–362, 2016.

[88] C. Koch, *Biophysics of Computation*. Oxford University Press, 1998, ISBN: 9780195104912.

[89] G. J. Stuart and B. Sakmann, "Active propagation of somatic action potentials into neocortical pyramidal cell dendrites," *Nature*, vol. 367, no. 6458, pp. 69–72, 1994.

[90] A. Wächter and L. T. Biegler, "On the implementation of an interior-point filter line-search algorithm for large-scale nonlinear programming," *Mathematical Programming*, vol. 106, no. 1, pp. 25–57, 2006.

[91] B. A. Toth, M. Kostuk, C. D. Meliza, D. Margoliash, and H. D. I. Abarbanel, "Dynamical estimation of neuron and network properties I: Variational methods," *Biological Cybernetics*, vol. 105, no. 3-4, pp. 217–237, 2011.

[92] M. Kostuk, B. A. Toth, C. D. Meliza, D. Margoliash, and H. D. I. Abarbanel, "Dynamical estimation of neuron and network properties II: path integral Monte Carlo methods," *Biological Cybernetics*, vol. 106, no. 3, pp. 155–167, 2012.

[93] A. Gupta, "WSMP: Watson Sparse Matrix Package Part I – direct solution of symmetric sparse systems," *WSMP: Watson Sparse Matrix Package*, vol. 21886, no. 98462, 2000.

[94] W. M. Kistler, W. Gerstner, and J. L. van Hemmen, "Reduction of the Hodgkin-Huxley Equations to a Single-Variable Threshold Model," *Neural Computation*, vol. 9, no. 5, pp. 1015–1045, 1997.

[95] W. Gerstner and R. Naud, "How Good Are Neuron Models?" *Science*, vol. 326, no. 5951, pp. 379–380, 2009.

[96] C. Rossant, D. F. Goodman, J. Platkiewicz, and R. Brette, "Automatic fitting of spiking neuron models to electrophysiological recordings," *Frontiers in Neuroinformatics*, vol. 4, no. MAR, pp. 1–10, 2010.

[97] R. Naud, B. Bathellier, and W. Gerstner, "Spike-timing prediction in cortical neurons with active dendrites," *Frontiers in Computational Neuroscience*, vol. 8, no. August, pp. 1–8, 2014. arXiv: `arXiv:1311.3586v1`.

[98] D. A. Brown, "M-Current: From Discovery to Single Channel Currents," in *Slow Synaptic Responses and Modulation*, Tokyo: Springer Japan, 2000, pp. 15–26.

[99] Y. Tsubo, T. Kaneko, and S. Shinomoto, "Predicting spike timings of current-injected neurons," *Neural Networks*, vol. 17, no. 2, pp. 165–173, 2004.

[100] C. Knowlton, S. Kutterer, J. Roeper, and C. C. Canavier, "Calcium dynamics control K-ATP channel-mediated bursting in substantia nigra dopamine neurons: A combined experimental and modeling study," *Journal of Neurophysiology*, vol. 119, no. 1, pp. 84–95, 2018.

[101] S.-M. Lee, J.-E. Kim, J.-H. Sohn, H.-C. Choi, J.-S. Lee, S.-H. Kim, M.-J. Kim, I.-G. Choi, and T.-C. Kang, "Down-regulation of delayed rectifier K+ channels in the hippocampus of seizure sensitive gerbils," vol. 80, no. 6, pp. 433–442, Dec. 2009.

[102] J. C. Wester and D. Contreras, "Biophysical mechanism of spike threshold dependence on the rate of rise of the membrane potential by sodium channel inactivation or subthreshold axonal potassium current," *Journal of Computational Neuroscience*, vol. 35, no. 1, pp. 1–17, 2013.

[103] B. Fontaine, J. L. Peña, and R. Brette, "Spike-Threshold Adaptation Predicted by Membrane Potential Dynamics In Vivo," *PLoS Computational Biology*, vol. 10, no. 4, pp. 1–11, 2014.

[104] H. Kuba and H. Ohmori, "Roles of axonal sodium channels in precise auditory time coding at nucleus magnocellularis of the chick," *Journal of Physiology*, vol. 587, no. 1, pp. 87–100, 2009.

[105] D. A. McCormick and A. Williamson, "Convergence and divergence of neurotransmitter action in human cerebral cortex.," *Proceedings of the National Academy of Sciences*, vol. 86, no. 20, pp. 8098–8102, 1989.

[106] E. C. Johnson, D. L. Jones, and R. Ratnam, "Minimum squared-error, energy-constrained encoding by adaptive threshold models of neurons," *2015 IEEE International Symposium on Information Theory (ISIT)*, pp. 1337–1341, 2015.

[107] C. M. Lee, A. F. Osman, M. Volgushev, M. A. Escabí, and H. L. Read, "Neural spike-timing patterns vary with sound shape and periodicity in three auditory cortical fields," *Journal of Neurophysiology*, vol. 115, no. 4, pp. 1886–1904, 2016.

[108] R. Jolivet, F. Schürmann, T. K. Berger, R. Naud, W. Gerstner, and A. Roth, "The quantitative single-neuron modeling competition," *Biological Cybernetics*, vol. 99, no. 4-5, pp. 417–426, 2008.

[109] W. Bair and C. Koch, "Temporal Precision of Spike Trains in Extrastriate Cortex of the Behaving Macaque Monkey," *Neural Computation*, vol. 8, no. 6, pp. 1185–1202, 1996.

[110] H. Mino, J. T. Rubinstein, and J. A. White, "Comparison of algorithms for the simulation of action potentials with stochastic sodium channels," *Annals of Biomedical Engineering*, vol. 30, no. 4, pp. 578–587, 2002.

[111] F. Farkhooi, M. F. Strube-Bloss, and M. P. Nawrot, "Serial correlation in neural spike trains: Experimental evidence, stochastic modeling, and single neuron variability," *Physical Review E*, vol. 79, no. 2, p. 021 905, 2009.

[112] R. F. Fox and Y. N. Lu, "Emergent collective behavior in large numbers of globally coupled independently stochastic ion channels," *Physical Review E*, vol. 49, no. 4, pp. 3421–3431, 1994.

[113] M. J. Chacron, B. Lindner, and A. Longtin, "Threshold fatigue and information transfer," *Journal of Computational Neuroscience*, vol. 23, no. 3, pp. 301–311, 2007.

[114] N. V. Marrion, "Control of M-current.," *Annual review of physiology*, vol. 59, no. 1, pp. 483–504, 1997.

[115] B. A. Bicknell and G. J. Goodhill, "Correction: Emergence of ion channel modal gating from independent subunit kinetics," *Proceedings of the National Academy of Sciences of the United States of America*, vol. 113, no. 51, E8357, 2016.

[116] G. S. Yi, J. Wang, H. Y. Li, X. L. Wei, and B. Deng, "Metabolic energy of action potentials modulated by spike frequency adaptation," *Frontiers in Neuroscience*, vol. 10, no. NOV, pp. 1–19, 2016.

[117] I. Siekmann, J. Sneyd, and E. J. Crampin, "Statistical analysis of modal gating in ion channels," *Proceedings of the Royal Society A: Mathematical, Physical and Engineering Sciences*, vol. 470, no. 2166, 2014.

[118] H. D. I. Abarbanel, D. R. Creveling, R. Farsian, and M. Kostuk, "Dynamical State and Parameter Estimation," *SIAM Journal on Applied Dynamical Systems*, vol. 8, no. 4, pp. 1341–1381, 2009.

[119] C. Varela, D. A. Llano, and B. B. Theyel, "An Introduction to In Vitro Slice Approaches for the Study of Neuronal Circuitry," in *Proceedings of the 2013 NAACL HLT Demonstration Session*, December 2011, 2011, pp. 103–125.

[120] C. M. Armstrong and F. Bezanilla, "Inactivation of the Sodium Channels. II Gating Current Experiments," *J Gen Physiol*, vol. 70, pp. 567–590, 1977.

[121] P. Pfeiffer, A. V. Egorov, F. Lorenz, J. H. Schleimer, A. Draguhn, and S. Schreiber, "Clusters of cooperative ion channels enable a membrane-potential-based mechanism for short-term memory," *eLife*, vol. 9, pp. 1–27, 2020.

[122] B. Naundorf, F. Wolf, and M. Volgushev, "Unique features of action potential initiation in cortical neurons," *Nature*, vol. 440, no. 7087, pp. 1060–1063, 2006.